NTNU

Norwegian University of
Science and Technology

Analyses of Two Ice Class Rules

for The Design Process of a Container Ship

Yixiang Su

Maritime Engineering
Submission date: June 2017
Supervisor: Bernt Johan Leira, IMT
Co-supervisor: Anders Ulfvarson, KTH

Norwegian University of Science and Technology
Department of Marine Technology

Master's Thesis in Nordic Master of Maritime Engineering

Analyses of Two Ice Class Rules

for The Design Process of a Container Ship

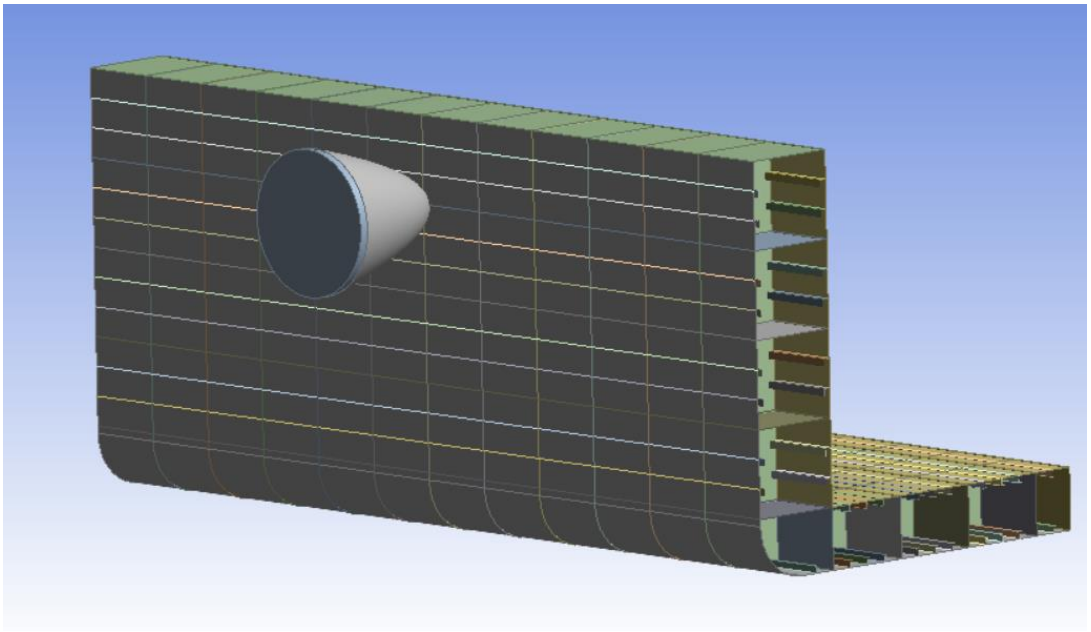

YIXIANG SU

Supervisor: Bernt Johan Leira

Norwegian University of Science and Technology, Trondheim, Norway

Department of Marine Technology

Co-supervisor: Anders Ulfvarson

Royal Institute of Technology, Stockholm, Sweden

Department of Aeronautical & Vehicle Engineering,

Abstract

During ice voyages, level ice and iceberg with huge inertia force can cause large deformation and even damage on the ship hull structure. Hence the hull structure for ice voyage requires higher strength than it for open water voyages.

A container ship will be re-designed for ice voyages in the thesis. Generally, the ice strength is evaluated in ice class rules. IACS polar class and FSICR are adopted in this thesis. Ice class rules are based on experience and experiment data, but there has been no exact formula or parameters to described the ice properties so far. In other words, the results from ice class rules include uncertainties.

In order to improve physical understanding, non-linear FE simulations will be processed after the re-design. In the simulations, the ship has a collision with different ice scenarios. The simulations are carried on ANSYS Workbench Explicit Dynamic using the solver of Auto-dyna. Afterwards, the results from the two designs schemes are compared and analysed.

Key words: IACS polar class, FSICR, Ice -ship collision, non-linear FE modelling, ANSYS

Preface

This report is the result of the Master's Thesis conducted by student Yixiang Su in spring 2017 at the Norwegian University of Science and Technology (NTNU). And it is a requirement for Nordic Master's Degree in Maritime Engineering at Royal Institute of Technology (KTH) and Norwegian University of Science and Technology (NTNU). The work is the continuation of the Master Project carried out in fall 2016. In the project, the basic designs from both ice class rules have been finished as well as a simple static analysis. More detailed designs are carried out in the thesis.

I tried both ANSYS Workbench and LS-DYNA as the simulation software at first. I had done some simple simulations on both software. The former one was simpler to use and its GUI interface was more intuitive. Besides, ANSYS Workbench had integrated the solver of LS-DYNA. Hence, I decided to use ANSYS Workbench finally.

The dynamic simulation was totally new to me. I studied it through a lot of tests and failures. At first, there were some errors on models. I improved and optimized it gradually, and started to be familiar with the modeling process. Then, I met challenges of input parameters. I had no idea about any parameters e.g. the most important two parameters: cycle numbers and termination time. I had to use the default ones. But the results were disappointed. With the ANSYS help viewer, I started to tried different input parameters to see the changes of results. I only set some small numbers at first. As a result, the results was disappointed. Finally, I knew that these two parameters restricted each other. The longer termination time, the more cycle number was needed.

I gained great progress in the process. With limited help, it would take me some hours or even some days to deal with simple problems at first. I had to learn the software and theory through papers, videos, forums and the user guide. And at the later stage, one single computation would cost around 10 hours. If there were some wrong inputs, almost one day's work would become none.

I received many suggestions and helps during the process of my thesis work. Firstly, I would like to thank my supervisor Professor Bernt Johan Leira at the Department of Marine

Technology in NTNU, for his directional guidance. And co-supervisor Professor Anders Ulfvarson at the Aeronautical and Vehicle Engineering in KTH. For his helps and advises through the whole procedure, and his suggestions on my paper work. Secondly, I would appreciate the help from Chi Chen, a graduate from Charmers University of Technology. He gave me constructive suggestions on the modelling and simulations.

Finally, I would say I have enjoyed the two years' fantastic life in Nordic countries. I am really honored to be a student in Nordic Master in Maritime Engineering. Thanks to the coordinators Paul Anderson **(**Technical University of Denmark), Anders Rosén (KTH) and Svein Sævik (NTNU).

Thirdly, I would thank for the supports from family and friends.

Trondheim, June 2017

Yixiang Su

Table of Content

Notations

Abbreviations

DNV GL	Det Norske Veritas (Norway) and Germanischer Lloyd (Germany).
IACS PC	International Association of Classification Societies Polar Class
FSICR	the Finnish-Swedish Ice Class Rules
PC	Polar Class
IMO	International Maritime Organisation
CAD	Computer Aided Design
CFL	Courant-Friedrichs-Lewy
PSF	Plastic Strain Failure

1 Background

1.1 Introduction

Ships and shipping industry has always been the most important way of transportation since they were invented. Because of the economic efficiency, almost 90% of the globally transported cargo is held in containers[1]. As a result, the container shipping industry plays the key role for transportation. Besides, the globalization and international trade boot the demand for large and specially designed vessels.

As a new opportunity arises, one more terminal, Helsinki (Finland), will be added to the scenario of an 800TEU feeder ship[2], the parent ship in this thesis, whose original route is from Oxelösund (Sweden) to Hamburg (Germany). The original hull structure design[3] has been finished followed by DNV GL rules[4].

Figure 1-1 Feeder ship

The Baltic Sea is one of the busiest transportation area in the world. There is no exception in winter. The ice forms in winter and melts in summer. Only first year level ice and some ice ridges will be taken into account. The ship structures for ice voyages will be designed according to ice class rules.

Figure 1-2 Baltic Sea transportation map(http://www.st-petersburg-essentialguide.com)

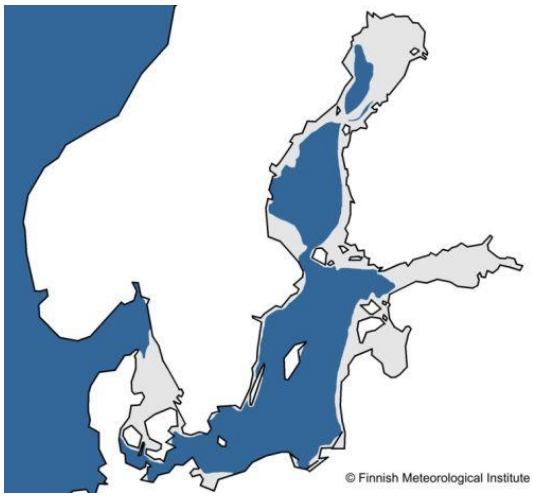

Figure 1-3 The largest ice extent in Baltic Sea, February 2012 (http://www.helcom.fi)

1.2 Objective

The main objective of this thesis is to analyses and draw conclusions from the application of two ice class rules for the design process of a container vessel.

1.3 Method

Firstly, based on the parent ship, a new set of scantling of the ship will be designed according to two different ice class rules. Then, to go deeper the understanding of the hull-ice interaction,

a simulation will be done. Non-linear FE modelling will be used. Finally, the results of the scantling with two ice class designs will be compared and analyzed.

1.4 Literature survey

For cargo transportation, containerships are ubiquitous. Today's giant containerships typically operate between purpose-built ports served by massive cranes that can load and unload containers at astonishing rates[1].

Cargos need to be transported all over the world, including the areas with ice coverage in winter. Helsinki is one of the most important and busiest port in Baltic Sea, whose port is all ice bound in winter[5]. Then the requirement of ship strength for ice voyage is essential. Ice strengthing ships are designed based on ice class rules. The first Finnish rules for winter navigation was published in 1890. And it is developed over time. In 1971, the Finnish-Swedish Ice Class Rules was set, and it has been accepted widely from then on. Besides, IACS Polar Class Rules are becoming more and more accepted, especially for multi-year ice conditions[7].

In class rules, structural requirements are based on a combination of experience, empirical data and structural analyses[7]. Not a few people have concluded their own empirical formulas. To summarize, displacement and speed of the ship are the two main factor that influence the global ice load. While for local ice pressure, the contact area is the main factor[6]. The selected ice rules share the same and clear definitions of the ice load.

For the FE simulation part, the collision theory has been perfected. Energy balance method is the general method[12]. In the process, the ice material properties are an important part. Ice properties changes with environment conditions, such as temperature, salinity, molecular structure and etc. Thus, there is no absolute definition of ice properties. But a lot of experiment have been done, the relative data have been summarized. and Haynes (1978)[18] did a series of test of the temperature influence on ice, and summarized the strength range of ice in one certain temperature. Besides, Liu (2010) put forward the Tsai-Wu yield surface of ice, which illustrated the plastic property of ice. The author succeeded doing the simulation in LS-Dyna, and the results is almost the same as the results from test. As for the material for hull structure, DNV

GL[4][14][16] have set the standard. During a collision process, the steel deformation may exceed the yield strength. Thus, a whole strain & stress relationship is supposed to be used. But the definition of failure should be discussed in detail. Ehlers (2012) [19] summarized the failure criteria related with the mesh size. The author illustrated that the failure strain decreases as element length increases.

Based on the theory above, Liu (2014)[10], Dong (2016)[11] and many other authors have succeeded simulating the collision process using Non-linear FE analysis.

1.5 Ice class rules selection

Different ice classes rules have been developed by nations traditionally. In mid-90s, IACS decided to develop unified polar ice class rules[7]. And now, not a few national ice classes rules are developed based on this. Thus its application range is wide. In other words, it is more general than other class rules.

The Finnish-Swedish Ice Class Rules (FSICR) are developed by The Finnish Transport Safety Agency and the Swedish Transport Agency since 1890. After centers of development, it has become an integral part of the winter navigation system. About 10000 ship visits test the rule strength and ice performance levels, and ends up with few damages[5].

The Ice Class Rules of the Russian Maritime Register of Shipping is more detailed than IACS polar class e.g. more ice conditions are defined. Unfortunately, it is now under development.

Other classification societies such as ABS (American Bureau of Standards) and LR (Lloyd's Register of Shipping) have their own ice rules. But they are not too related for this thesis.

Only ICAS polar class and FSICR are used for this thesis.

1.6 Procedures

Firstly, according to the ice rules, the ice class needs to be decided. There are 7 levels in IACS polar class and 4 levels in FSICR. All the following steps are based on ice class. As mentioned in Chapter 1.1, Only first year level ice and some ice ridges will be taken into account,

corresponding to IACS PC 7 and FSICR IC class.

Secondly, combined with the dimensions of the parent ship, the value of ice load can be calculated.

Thirdly, new scantling can be designed according to the calculated ice load.

Fourthly, the simulation can start. The hull part and the ice part will be non-linear modelled respectively. The scantling with one ice class rule will be used first, and the scantling from the other rule will be used afterwards. In reality, the collision conditions (area, speed, shape and angle) is random. Hence, some simplification will be taken to save time, which will be discussed later.

Lastly, the results from two designs will be compared. The results analysis will focus on the damage area, large deformation as well as the maximum equivalent strain and energy.

The procedure is showed in Figure 1-4.

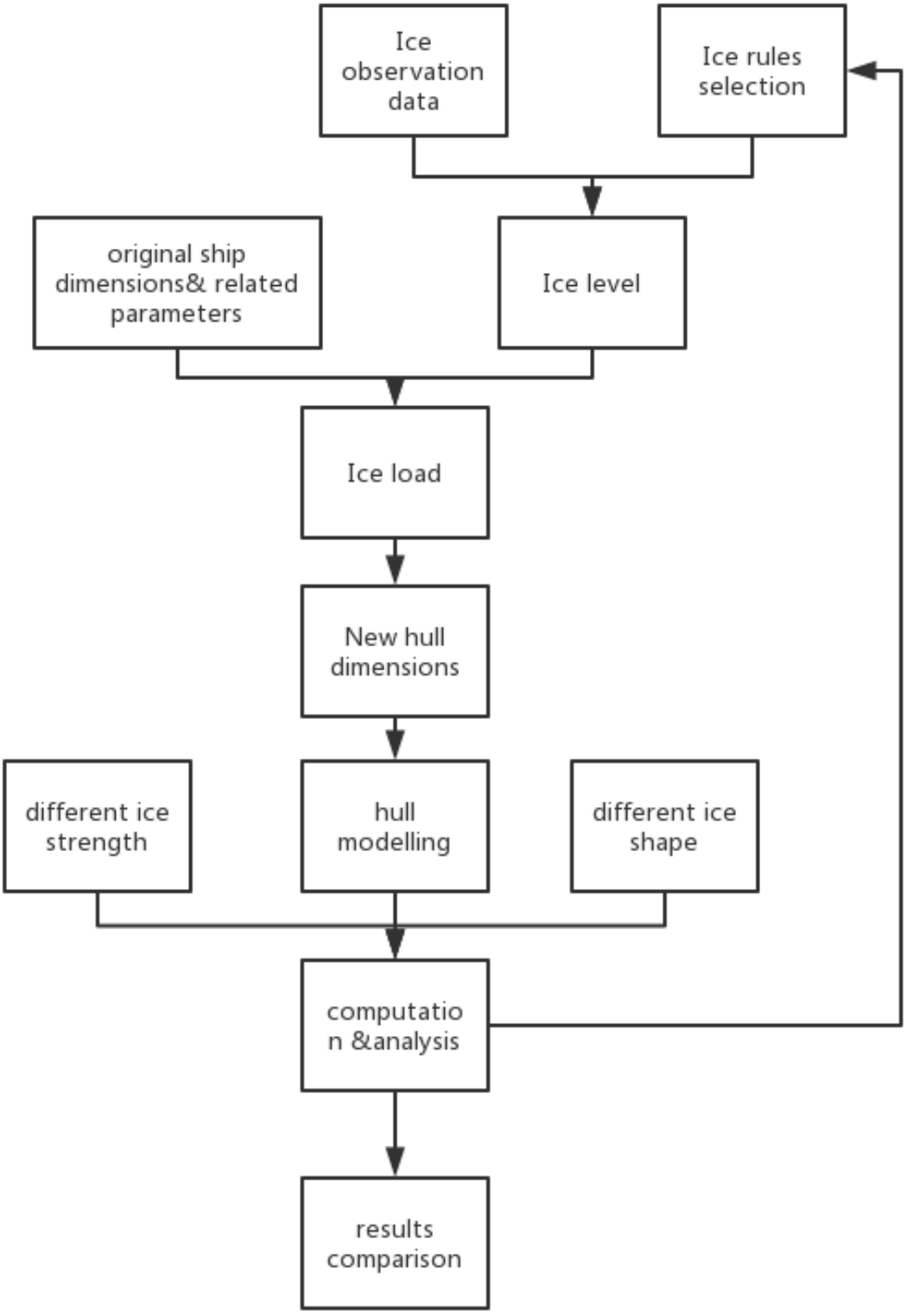

Figure 1-4 Design procedure

2 Ice class rules calculation

The two selected ice class rules will be applied to the design of the parent ship, IACS polar class and FSICR.

2.1 Initial ship dimensions

The parent ship is an 800TEU feeder ship with a design speed of 18.9kn. The ship complies with the intact stability criteria, issued by IMO. Its main measurements are listed in Table 2-1.

Table 2-1 Ship Mean measurement

Object	Value
Length over all, L_{oa}[m]	130.65
Length between perpendiculars, L_{pp} [m]	125.3
Width, Beam[m]	22.88
Draught, d[m]	7.05
Scantling draught, T_{scant} [m]	9.34
Freeboard, F[m]	4.31
Depth to main deck, D[m]	11.36
Height overall, H_{oa}[m]	29.96
Block coefficient, CB	0.63
Cruising speed, VS[kn]	18
Engine output, P_{inst}[kW]	10800
Displacement, Δ[t]	13457
Deadweight, DW[t]	9611
Lightweight, LW[t]	3846
Ballast water, loaded ship BW_{loaded}[t]	0
Ballast water, empty ship BW_{empty}[t]	2153
Cargo capacity[TEU]	809

(Continued Table 2-1)

Object	Value
Containers number in holds[TEU]	267
Containers number on deck[TEU]	542
Vertical center of gravity, KG[m]	9.32
Longitudinal center of gravity, LCG[m]	58.9
Metacentric height, GMO[m]	1.59

The hull structure for open water voyage is finished. All the scantlings comlies with DNV GL rules for hull structure. Its strength for open water scenario (full loaded and in ballast) has already been verified. Figure 2-1 showed the cross section CAD model. The detailed dimensions for hull side part are listed in Table 2-2, which will be used for ice strength calculating.

Table 2-2 Side structure dimensions

Object		value
plate	Outer plate thickness [mm]	15
	Inner plate thickness[mm]	15
spacing	Girder spacing [mm]	2415
	Longitudinal [mm]	805
	Floor[mm]	2125
Longitudinal	web height [mm]	200
	web thickness [mm]	80
	flange width [mm]	200
	flange thickness[mm]	80
	section modulus [cm3]	414
girder	thickness	11
	section modulus [cm3]	12972
Dimensions	Hull length [m]	25.5

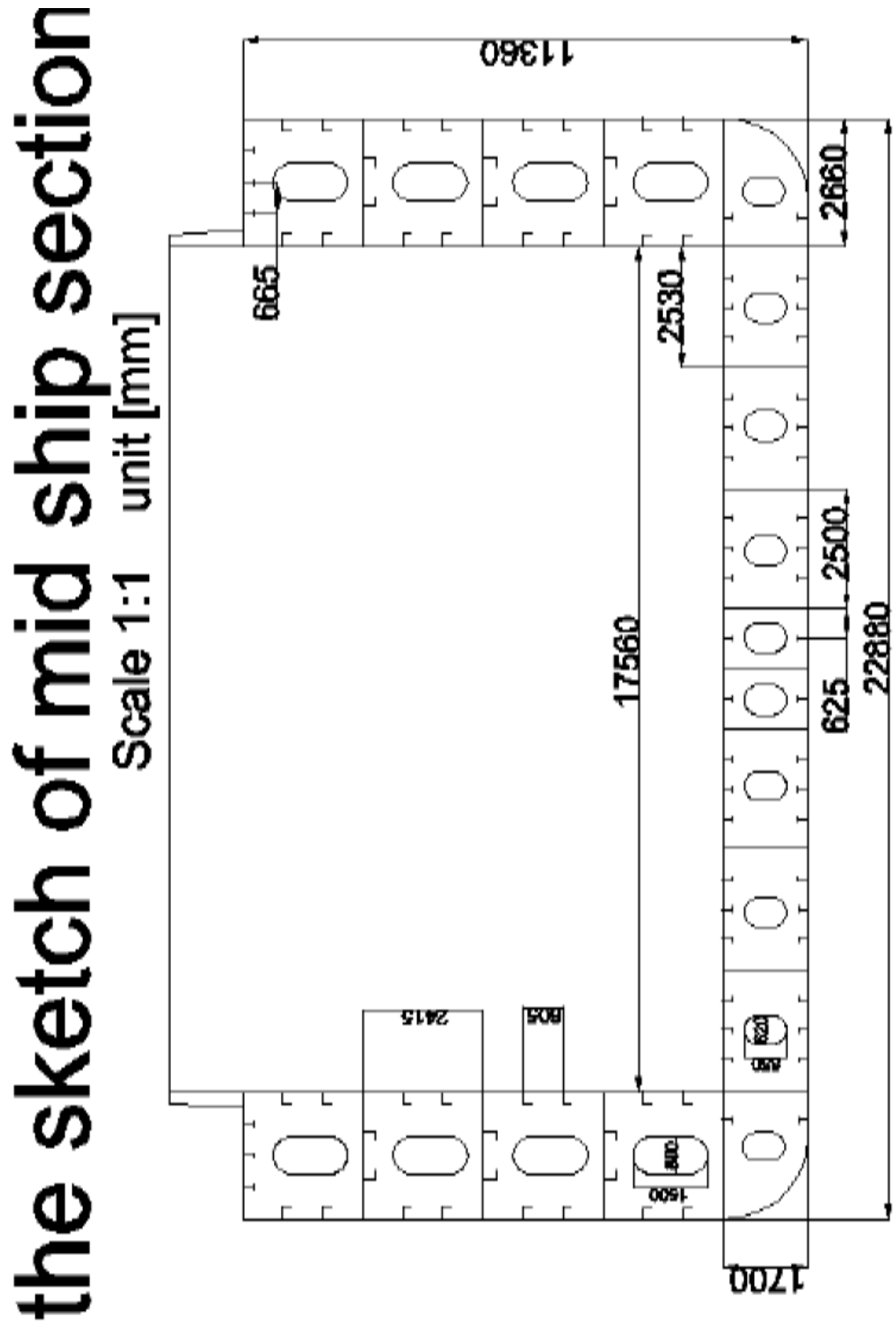

Figure 2-1 Hull structure cross section

2.2 IACS polar class calculation

2.2.1 Ice class

There are 7 levels of ice class in IACS PC. In this thesis, PC 7 is selected for this thesis[8].

Table 2-3 Polar class description

Polar Class	Ice descriptions (based on WMO Sea Ice Nomenclature)
PC 1	Year-round operation in all polar waters
PC 2	Year-round operation in moderate multi-year ice conditions
PC 3	Year-round operation in second-year ice which may include multiyear ice inclusions.
PC 4	Year-round operation in thick first-year ice which may include old ice inclusions
PC 5	Year-round operation in medium first-year ice which may include old ice inclusions
PC 6	Summer/autumn operation in medium first-year ice which may include old ice inclusions
PC 7	Summer/autumn operation in thin first-year ice which may include old ice inclusions

2.2.2 PC 7 parameters

The parameters defining the glancing impact load characteristics for PC 7 are reflected in the Class Factors listed in Table 2-4.

Table 2-4 IACS PC 7 related parameters

Description	Symbol	value
Crushing failure class factor	CF_C	1.8
Flexural failure class factor	CF_D	4.06
Load patch dimension class factor	CF_D	1.11
Displacement class factor	CF_{DIS}	22
Longitudinal strength class factor	CF_L	1.81

(Continued Table 2-4)

Description	Symbol	value
Crushing failure class factor	CF_{CV}	2.6
Line load class factor	CF_{QV}	2.33
Pressure class factor	CF_{PV}	0.65
Hull area factor	M_i	0.48

2.2.3 Ice pressure

According to I2.3.2, the ice pressure and load patch can be calculated:

(a) Force:

$$F_{NonBow} = 0.36 CF_C DF [MN] \quad \text{eq. 2-1}$$

DF: ship displacement factor

$=D^{0.64}$ if $D \leqslant CF_{DIS}$

$=CF_{DIS}^{0.64} + 0.1(D - CF_{DIS})$ if $D > CF_{DIS}$

D: ship displacement [kt].

(b) Line load:

$$Q_{NonBow} = 0.639 F_{NowBow}^{0.61} CF_D \ [MN/m] \quad \text{eq. 2-2}$$

(c) Design load patch:

$$w_{NonBow} = F_{NonBow}/Q_{NonBow} \quad \text{eq. 2-3}$$

$$b_{\boldsymbol{NonBow}} = w_{NonBow}/3.6 \quad \text{eq. 2-4}$$

w_{NonBow}: load patch width [m];

b_{NonBow}: load patch height [m].

(d) Ice pressure:

$$p_{avg} = F_{NonBow}/(b_{\boldsymbol{NonBow}} w_{NonBow}) \quad \text{[Mpa]} \quad \text{eq. 2-5}$$

(e) Result:

Table 2-5 load patch and ice pressure

Description	Symbol	value
width [m]	l	2.27
height [m]	h	0.63
Pressure[Mpa]	P_{avg}	2.37

2.2.4 Hull thickness of ice belt

According to I2.4, the plate thickness can be calculated. For b<s:

$$t_{net} = 500 \cdot s\left(\frac{AF \cdot PPF_P \cdot p_{avg}}{\sigma_y}\right)^{0.5} \cdot \left(2 \cdot \frac{b}{s} - \left(\frac{b}{2}\right)^2\right)^{0.5} / (1 + \frac{s}{2 \cdot l \cdot}) \text{ [mm]} \qquad \text{eq. 2-6}$$

b: height of design load patch;

s: transvers frame spacing;

σ_y: material yield strength;

l: distance between frame support.

The results are listed in Table 2-6.

Table 2-6 Hull thickness from IACS

Description	Symbol	value
Net height [mm]	T_{net}	34.9
Corrosion allowance [mm]	T_s	2.5
Required plate thickness[mm]	T	37.4
Design plate thickness[mm]	T	38

Because of the different load condition of the ship, for conservative design, the height of this plate is set from 7m to 10m from the base line, shown in Figure 2-2.

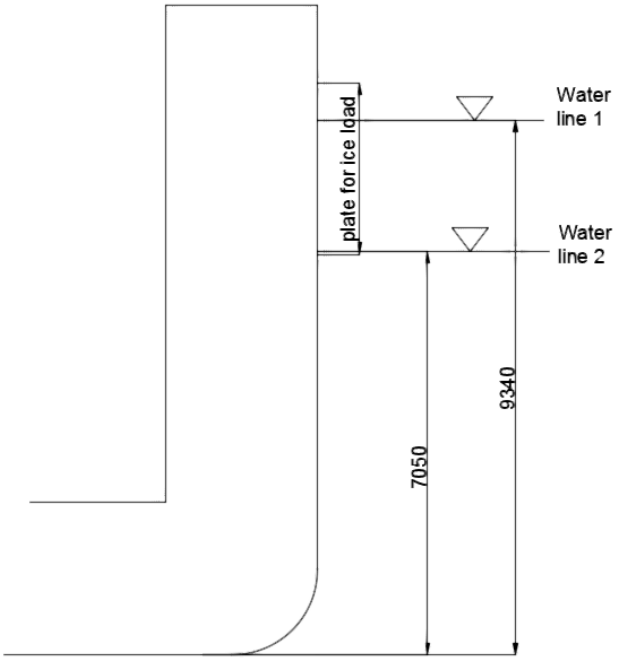

Figure 2-2 Plate height for ice load

2.2.5 Longitudinal

The minimum effective shear area of the longitudinals is given in I2.7.2:

$$A_L = 100^2(AF \cdot PPF_S \cdot p_{avg}) \cdot 0.5 \cdot b_1 \cdot a/(0.577 \cdot \sigma_y) \text{ [cm}^2\text{]} \quad \text{eq. 2-7}$$

AF: hull area factor, equals to 0.45 here;

$b_1 = k_0 \cdot b_2$;

$k_0 = 1 - 0.3b/s$;

b: load patch height;

s: load patch width.

a: effective span of longitudinal local frame.

And the minimum effective plastic section modulus is given in I2.7.3:

$$Z_{pl} = 100^3 \cdot (AF \cdot PPF_S \cdot p_{avg}) b_1 \cdot a^2 \cdot A_4/(8\sigma_y) \text{ [cm}^3\text{]} \quad \text{eq. 2-8}$$

$A_4 = \frac{1}{2} + k_{wl} \cdot [(1 - a_4{}^2)^{0.5} - 1])$;

$a_4 = A_L/A_W$;

A_L: minimum shear area for longitudinal [cm^2];

A_W: net effective shear area of longitudinal [cm^2];

$k_{wl} = 1/(1 + 2 \cdot A_{fn}/A_W)$;

A_{fn}: net cross-sectional area of local frame flange.

These values as well as the designed values are listed in Table 2-7.

Table 2-7 Required longitudinal dimensions from IACS

Section modulus	value
Required minimum section modulus[cm^3]	376
Design section modulus[cm^3]	414[1]

The cross section of longitudinal is shown in the Figure 2-3.

[1] Here the longitudinal keeps the same as it for open water.

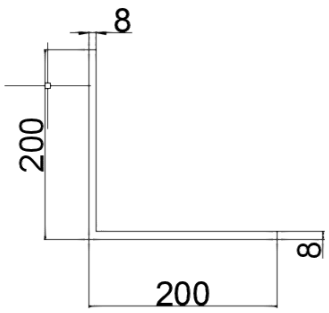

Figure 2-3 Longitudinal cross section [mm]

2.2.6 Web frame and stringers

According to I 2.9, the required thickness of stingers is:

$$t_{wn} = 2.63 \cdot 10^{-3} \cdot c_1 \left(\frac{\sigma_y}{5.34+4\left(\frac{c_1}{c_2}\right)^2}\right)^{0.5} [\text{mm}] \qquad \text{eq. 2-9}$$

c1=hw - 0.8 · h [mm];

hw: web height of stringer / web frame [mm];

h: height of framing member penetrating the member under consideration [mm];

c2: spacing between supporting structure oriented perpendicular to the member under consideration [mm].

For girder, hw=2660, c2=2415, twn=41.5mm

For floor, hw=2660, c2= 2125, twn=38.5mm.

Table 2-8 Frame dimensions from IACS

Object	value
Girder thickness[mm]	41
Floor thickness[mm]	38

2.3 FSICR calculating

2.3.1 Ice class

Three regions are defined in FSICR, which are fore, mid and aft. In this thesis, only mid region is of interested[9]. And the ice belt is defined in Figure 2-4.

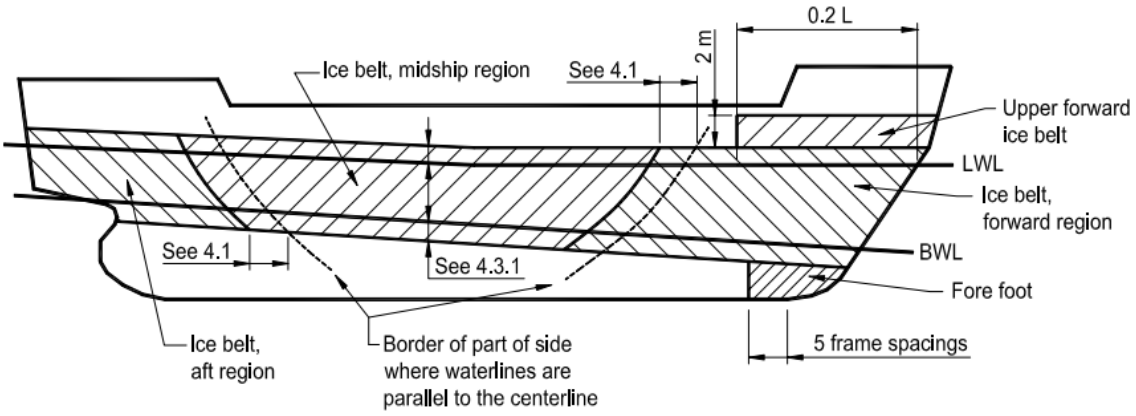

Figure 2-4 Hull structure regionalism

4 ice classes are introduced here according to the thickness of level ice.

Table 2-9 Height of load area

Ice class	h_0[m]	h[m]
IA super	1	0.35
IA	0.8	0.3
IB	0.6	0.25
IC	0.4	0.22

In Table 2-8, h_0 is the maximum level ice thickness, h is the designed height of the actual contact area. In this thesis, IC is adopted.

2.3.2 Ice pressure

According to 4.2.2 of the rules, the ice pressure can be calculated

$$P = c_d \cdot c_1 \cdot c_a \cdot p_0 \qquad \text{eq. 2-10}$$

c_d=0.279, is related with the engine output and the maximum displacement;

c_1=0.5;

c_a=0.474, is related with the frame spacing;

P_0=5.6Mpa, the nominal ice pressure.

Table 2-10 Ice load

Description	Symbol	value
Ice pressure[Mpa]	p	0.584
Total force on ice belt[MN]	F	3.27

Here, total force F equals to pressure times area[2].

2.3.3 Plate thickness

According to 4.3.2 of the rules, the plate thickness in ice belt for transverse framing ship can be calculated:

$$t = 667s\sqrt{\frac{P_{PL}}{f_2\sigma_y}} + t_c \qquad \text{eq. 2-11}$$

s=the frame spacing;

P_{PL}=0.75p;

f_2=9.38;

t_c=abrasion and corrosion allowance, shall be 2mm in FSICR.

the material is high-strength hull structural steel[3], whose yield strength is 355Mpa.

Table 2-11 Hull thickness from FSICR

Description	Symbol	value
Net height [mm]	t_{net}	31.4
Corrosion allowance [mm]	t_s	2
Required plate thickness[mm]	t	33.4
Design plate thickness[mm]	t	34

2.3.4 Longitudinals

For frame strength check, there would be vertical extension, defined in FSICR 4.4.1.

Table 2-12 Vertical extension of the ice strengthening

Ice class	Region	Above LWL[m]	Below BWL[m]
IC	Midship	1	1.3

The minimum section modulus defined by the rules (4.4.2.1):

$$Z = \frac{p \cdot s \cdot h \cdot l}{m_t \cdot \sigma_y} 10^6 \qquad \text{eq. 2-12}$$

m_t: a shape factor related with the boundary condition.

Table 2-13 Longitudinal modulus from FSICR

[2] In FSICR, the load area is defined all through the ice belt, which equals to hull length times designed height

Section modulus	value
Required minimum section modulus[cm^3]	382
Design section modulus[cm^3]	414

The section modulus of side shell longitudinal from initial design meet the requirement, so there is no need to update. The details are shown in Figure 2-3.

2.3.5 Web frame and stringers

According to 4.5.1, the required section modulus of stringers should follow:

$$Z = \frac{f_5 phl^2}{m\sigma_y} 10^6 \ [cm^3] \qquad \text{eq. 2-13}$$

The shear area shall be:

$$A = \frac{\sqrt{3} f_5 phl}{2\sigma_y} 10^4 [cm^2] \qquad \text{eq. 2-14}$$

m: boundary condition factor; to be taken as 13.3.

f5: factor which takes account of the distribution of load to the transverse frames; to be taken as 0.9.

Table 2-14 Frame dimensions from FSICR

Object	value
Girder thickness[mm]	31
Floor thickness[mm]	26

2.4 Comparison

From Table2-13, there is little difference of plate thickness and modulus requirement between the two ice class rules. Both results will be analyzed during the simulation.

Table 2-15 Results comparison between IACS and FSICR

Class	Ice pressure [Mpa]	Load area [m^2]	Total force [MN]	Plate Required thickness [mm]	Section modulus of stiffener[cm^4]	Girder thickness [mm]	Floor thickness [mm]
IACS	2.37	2.27x0.63	3.39	38	376	41	38
FSICR	0.587	25.5x0.22	3.27	34	382	31	26

The IACS rules depends only on the total displacement while the FSICR depends on the draught,

displacement and engine output. From the table above, the dimension differences are not significant. While the definition and value of ice pressure varies a lot. Obviously, IACS is much more severe for local strength.

3 Collision simulation theory

3.1 Ice load introduction

Generally, the extreme ice load will act on the bow part[6]. While for ship hull part, the ice load can also be critical. There will be ice compressive force action on the hull, shown in Figure 3-1. If the hull plate strength is not strong enough, the breakage can be destructive, followed by immeasurable loss. For new designed ships, the hull strength check is also important.

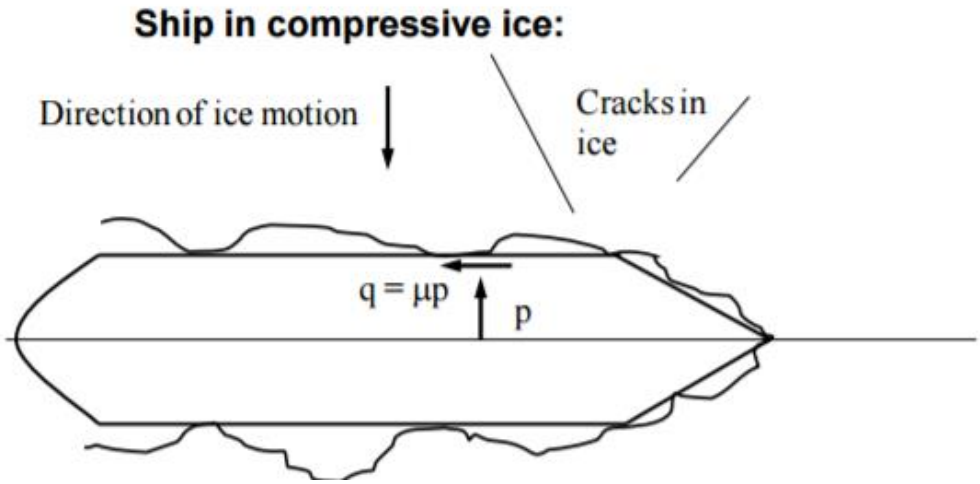

Figure 3-1 Compressive ice load actin on ship hull

Unlike the problem of ice resistance estimation, hull shape or ice properties are not considered to be important parameters in estimating the extreme ice load. The ice load depends on kinetic energy of the system. Even so, many different parameters can influence the ice strength such as hull angle and engine power. Unfortunately, it is not possible to include all the parameters when predicting. But some main parameters can be summarized and used. For global ice load, the displacement and ship speed are the main parameters. While for local ice load, the contact area is of interest. There are many different kinds of empirical formulas. But in this thesis, only formulas from class rules are used and only the local strength will be verified.

To verify the strength of the hull, the pressure on this area need to be calculated. In reality, the shape of this area is irregular. To simply the calculation, a regular rectangle load patch with height h and width l is defined, shown in Figure 3-2.

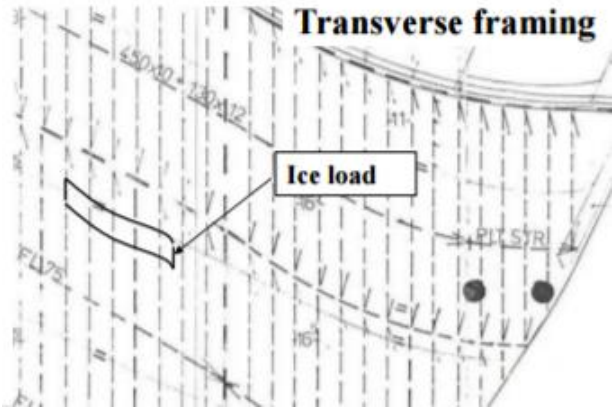

Figure 3-2 Irregular load area

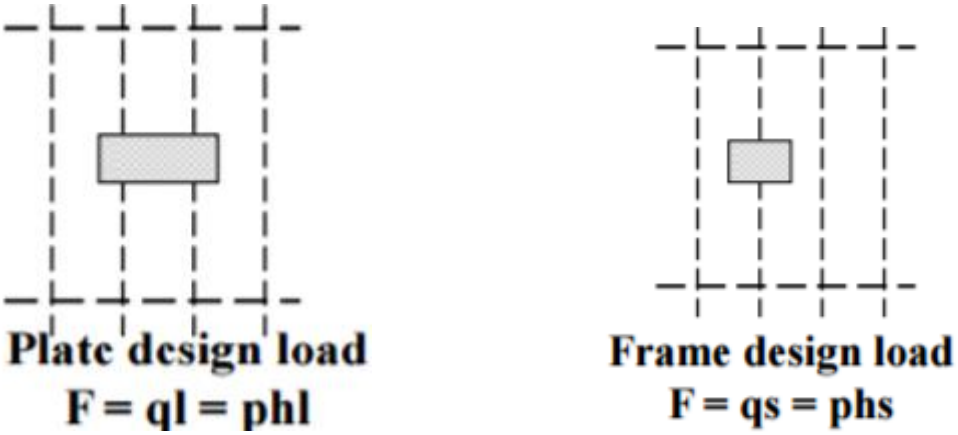

a. Load patch for plate check

b. Load patch for stiffener check

Figure 3-3 Ice load patch

The load patch should be positioned on corresponding location to check different components. For plates, the load patch is positioned between two stiffeners/frames (Figure 3-3 a). For stiffeners/frames, the symmetric axis of the load patch overlaps the stiffener of interest (Figure 3-3 b). It is the same with longitudinal.

During the calculating, the total force is assumed constant, shown in Figure 3-4 Thus, the average pressure inversely proportional to the load patch area:

$$p = \frac{F}{hl} \qquad \text{eq. 3-1}$$

F: total force;

h: height of ice load patch;

l: width of ice load patch.

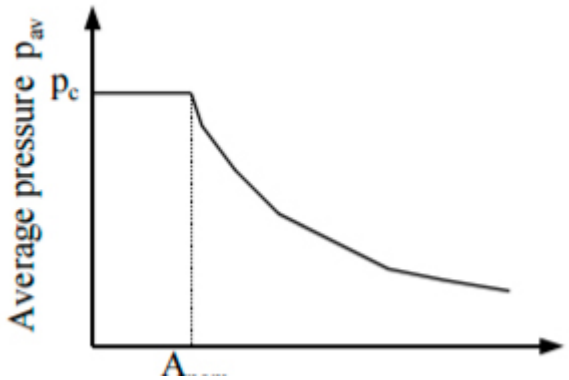

Figure 3-4 Average patch pressure with constant ice force

The same as sea loads, ice loads are also stochastic. While the probability of encountering higher ice loads is annually about 1%, and the magnitude is much higher than sea loads. The balance between economy and safety must be found. It is not economic to choose elastic design (linear materials) for the required excessively heavy structures. As a result, plastic design (non-linear materials) is used for ice loads.

3.2 Energy balance description

A collision simulation analysis is based on energy balance[10][11][12]. It can be adopted to ice-ship collision as well. It is assumed that one body is initially moving (the striking body) and the other is at rest (the struck body). To save computation time, in this thesis, the hull is fixed, and it is assumed the ice is initially moving. Thus, there is an initial kinetic energy for ice.

$$\mathrm{KE}_i = \frac{1}{2}\int dV \cdot v^2 \qquad \text{eq. 3-2}$$

dV: ice volume;

v: ice initial speed.

As the ice model moving, it starts contacting with the hull body (the ice load patch), and the crashing energy is generated. The available kinetic energy equals the sum of indentation energy and potential energy.

$$\mathrm{KE_e} = \mathrm{IE} + \mathrm{PE} \qquad \text{eq. 3-3}$$

KE_e: available kinetic energy;

IE: indentation energy;

PE: potential energy.

$$IE = \int_0^{\xi_m} F_n d_{\xi_c} \quad \text{eq. 3-4}$$

ξ_m: mass displacement;

ξ_c: crushing indentation displacement.

F_n: Indentation force.

$$PE = \int_0^{\xi_e} F_n d_{\xi_e} \quad \text{eq. 3-5}$$

ξ_e: recoverable displacement.

Because of the struck body of the hull, it cannot gain kinetic energy. In other words, the initial kinetic energy of ice equals to the available kinetic energy in this case. Eq. 3-2 can be solved foe F_n provided that the required kinematic and geometric values are known.

3.3 Explicit dynamic introduction

3.3.1 Explicit dynamic equations

The density at any time can be determined from the current volume of the zone and its initial mass[12]:

$$\frac{\rho_0 V_0}{V} = \frac{m}{V} \quad \text{eq. 3-6}$$

And the partial differential equations:

$$\begin{aligned} \rho\ddot{x} &= b_x + \frac{\partial \sigma_{xx}}{\partial x} + \frac{\partial \sigma_{xy}}{\partial y} + \frac{\partial \sigma_{xz}}{\partial z} \\ \rho\ddot{y} &= b_y + \frac{\partial \sigma_{yx}}{\partial x} + \frac{\partial \sigma_{yy}}{\partial y} + \frac{\partial \sigma_{yz}}{\partial z} \\ \rho\ddot{z} &= b_z + \frac{\partial \sigma_{zx}}{\partial x} + \frac{\partial \sigma_{zy}}{\partial y} + \frac{\partial \sigma_{zz}}{\partial z} \end{aligned} \quad \text{eq. 3-7}$$

The conversation energy:

$$\dot{e} = \frac{1}{\rho}(\sigma_{xx}\dot{\varepsilon_{xx}} + \sigma_{yy}\dot{\varepsilon_{yy}} + \sigma_{zz}\dot{\varepsilon_{zz}} + 2\sigma_{xy}\dot{\varepsilon_{xy}} + 2\sigma_{yx}\dot{\varepsilon_{yx}} + 2\sigma_{zx}\dot{\varepsilon_{zx}} \quad \text{eq. 3-8}$$

3.3.2 Explicit time integration

A nodal acceleration is:

$$\ddot{x}_\iota = \frac{F_i}{m} + b_i \qquad \text{eq. 3-9}$$

$\ddot{x}_\iota$: nodal acceleration (i=1,2,3);

F_i: force acting on the nodal points;

b_i: body acceleration;

m: nodal mass.

After determining the acceleration at time n, the velocity at time n+1/2 can be found from:

$$\dot{x}_i^{n+1/2} = \dot{x}_i^{n-1/2} + \ddot{x}_i^n \Delta t^n \qquad \text{eq. 3-10}$$

and the displacement at n+1 can be gained after integration:

$$\mathrm{x}_i^{n+1} = \mathrm{x}_i^n + \dot{x}_i^{n+1/2} \Delta t^{n+1/2} \qquad \text{eq. 3-11}$$

To ensure stability and accuracy of the solution, the time step used is constrained by the CFL condition in Workbench. This condition limits the time step can only travel within the smallest characteristic element dimension (mesh size) in a time step[12][16]. The time step criteria is:

$$\Delta \mathrm{t} \leq \mathrm{f} \cdot \left[\frac{h}{c}\right]_{min} \qquad \text{eq. 3-12}$$

Δt: the time increment;

f: the stability time step factor (= 0.9 by default);

h: the characteristic dimension of an element;

c: the local material sound speed in an element, for steel is 5200m/s

3.3.3 Solution process

The solution process starts with meshing, then the nodes are created. The initial conditions, such as velocity, acceleration, pressure and etc., will be applied to the nodes, and the time integration starts. The element will deform because of the nodal motions, which will create element strain rate. Then the stress can be calculated based on the strain & stress relationship, and the generated stress will act back on the nodes again. In the process, the nodal acceleration

can be calculated by the force and mass and will be integrated to get new velocity. Then a new iterate starts. Figure 3-5 shows the computation loop[13].

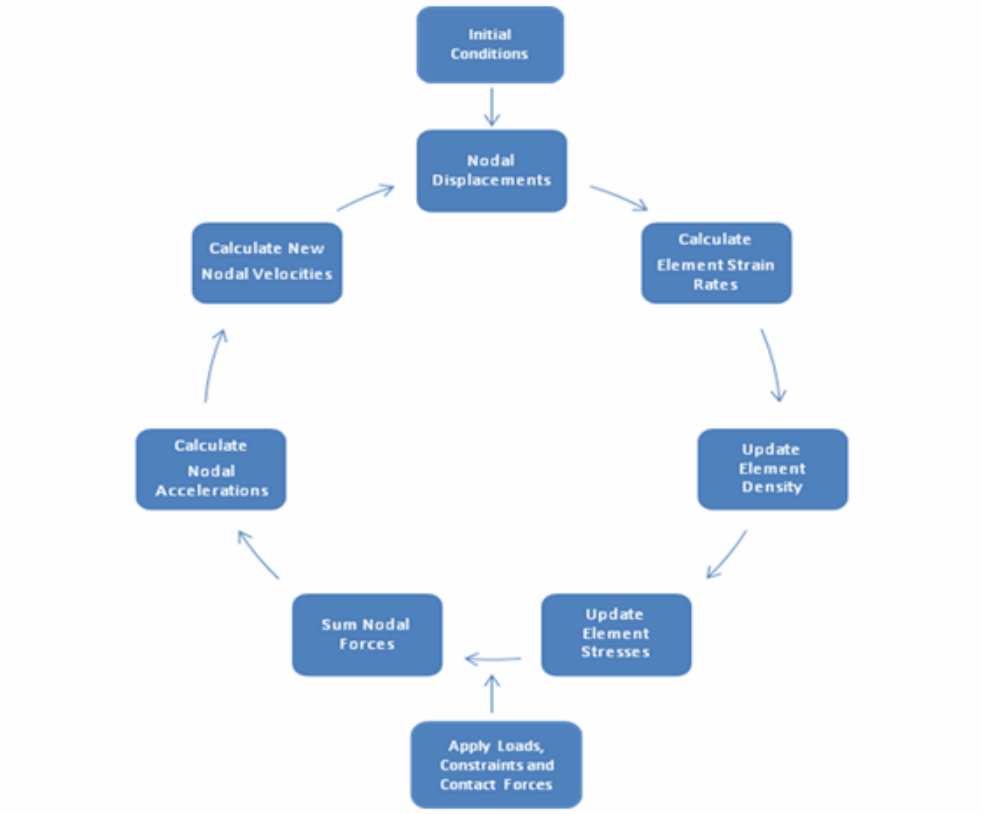

Figure 3-5 Explicit solution loop

3.4 Materials introduction

3.4.1 Steel material

The original materials for hull structure are listed in Table 3-1.

Table 3-1 Original materials for the hull

Steel	Yield strength [Mpa]	Structural members
NV-A36	355	shell plate, including keel, outer bottom and side plates, inner bottom, bottom longitudinal, girders
NV-NS	235	transvers members, including floors, web frames and plates for transvers bulkheads, longitudinal

Followed by DNV Rules[4][14] & IACS Polar Class[8], minimum material grades for ship hull

plate with ice strength is Grade A/BH. NV-A36 belongs to this grade. In this thesis, NV-A36 is also used for sub-structures.

NV-A steel is a high strength steel for marine structures. It is also widely used for ice strength ships. And its detailed properties are listed in Table 3-2.

Table 3-2 NV-A36 steel properties

Properties	Value
Density[kg/m3]	7850
Poisson's ration	0.3
Young's modulus[Ga]	210
yield strength[Mpa]	355

The strain/stress relationship in this simulation will come into plastic phase and even exceed the breaking strength. Hence, the simple linear relationship between strain and stress is not enough. The true strain is:

$$\varepsilon_{total} = \varepsilon_{elastic} + \varepsilon_{plastic} \qquad \text{eq. 3-13}$$

$\varepsilon_{elastic} = \sigma_f / E$;

σ_f: failure stress;

E: Young's modulus.

A whole stress & strain relationship curve will be adopted in this simulation (Figure 3-6).

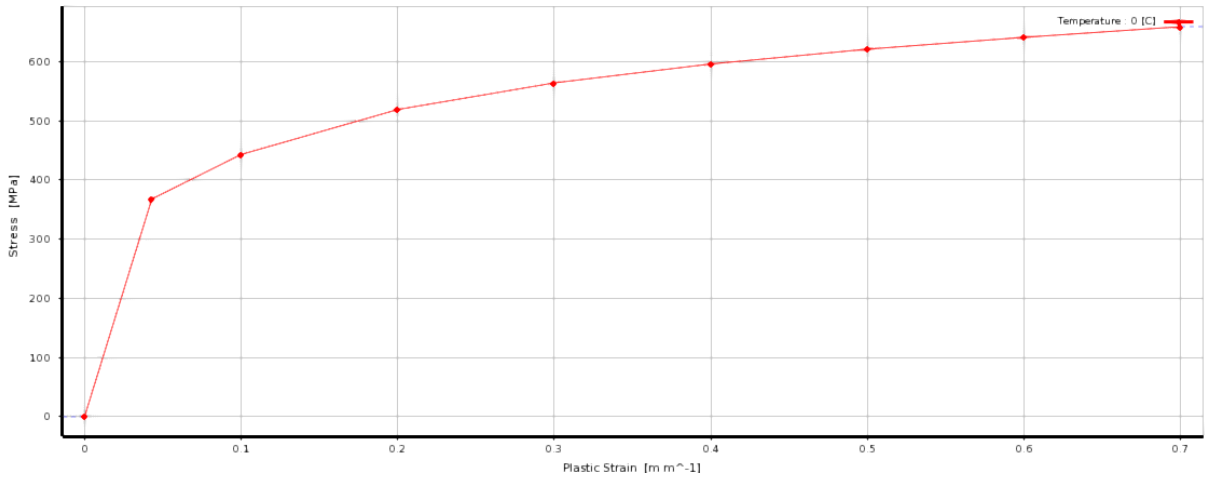

Figure 3-6 Stress & strain relationship of NV-A36 steel

For shell element, the only failure criterion is Plastic Strain Failure (PSF). Sören Ehlers (2012)[19] indicated that the maximum strain is related with the element size (Figure 3-7). According to the Table 3-3 , a fitting formula at 0℃ can be gained:

$$\varepsilon_{total} = l^{-0.2813} \quad \text{eq. 3-14}$$

l: element size[mm];

Figure 3-8 is the new plot. According to the results, when element size is 100mm (refers to Chapter 4.2), $\varepsilon_{total} = 0.27$.However, this value is the total strain rather the plastic strain. From Figure 3-6, when $\varepsilon_{total} = 0.27$, $\sigma = 570$Mpa, insert the value into eq. 3-13, the plastic failure can be calculated.

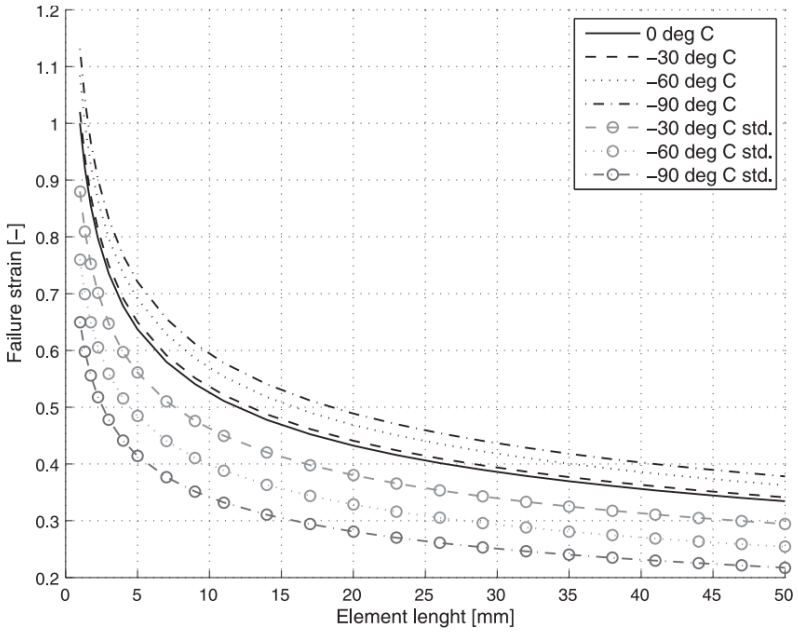

Figure 3-7 Relationship between failure strain and element length

Table 3-3 Relationship between strain failure and element length

Element length[mm]	strain
1	1
5	0.63
10	0.53
15	0.47
20	0..44
25	0.4
30	0.39
35	0.36
40	0.35
45	0.34

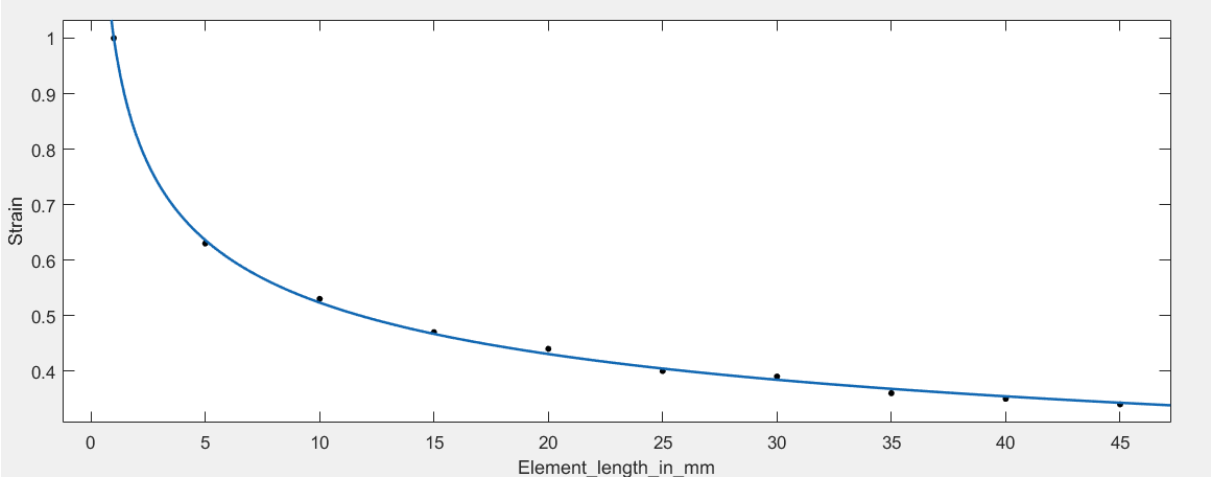

Figure 3-8 Fitting formula plot of element size & maximum strain relationship

3.4.2 Ice material

After investigation, the level ice class in this route is the lowest. As a result, it is not critical. Besides, the level ice is an ideal model. It reality, the ice shape is random. Other critical situations will be occurred by vessels e.g. ice ridges and icebergs. Hence, instead of level ice, some other more critical ice scenario e.g. iceberg will be taken into consideration. Apparently, the setting of ice property will influent the simulation results. However, the studies' results on ice have never been unified. The physical and mechanical properties of ice also change with many factors, such as temperature and salinity.

In general, the density of ice is around 900kg/m^3, and Young's modulus of ice is around 9Gpa to 10Gpa with Poisson's ration of around 0.3. The controversial part is its strength.

Liu (2010) [17]proposed a pressure-dependent and strain rate-independent ice model, in which Tsai-Wu yield surface was used. This simulation results of this model is close to the experiment results. Moreover, the ice strength changes a lot with temperature. Haynes (1978)[18] did the ice strength test with different temperature (Figure 3-9 & Figure 3-10). The ice strength increases as temperature decreases. To simplify the simulation, the temperature changes between the air and water is neglected. For ice in sea water, the temperature is around 0℃.

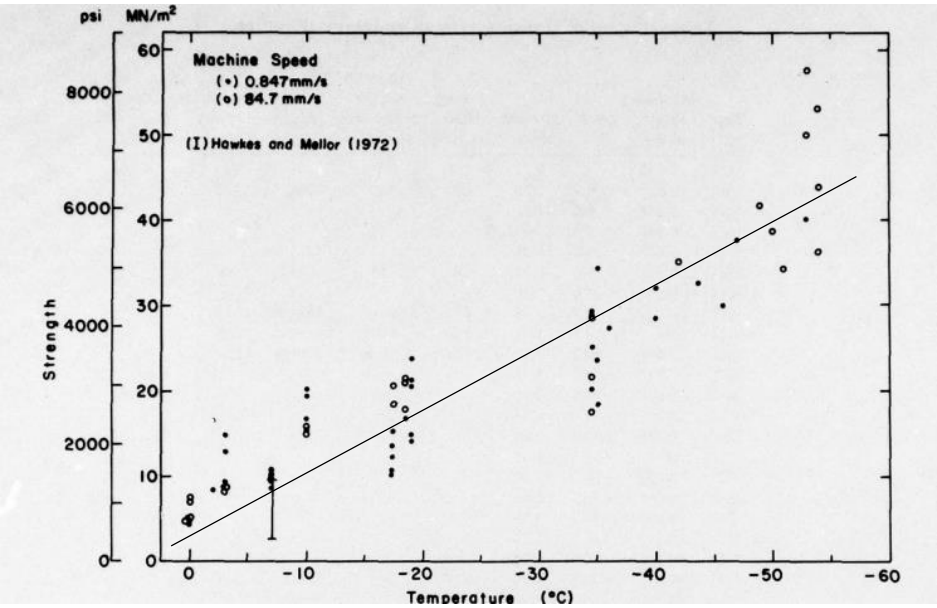

Figure 3-9 Ice compressive strength with temperature[18]

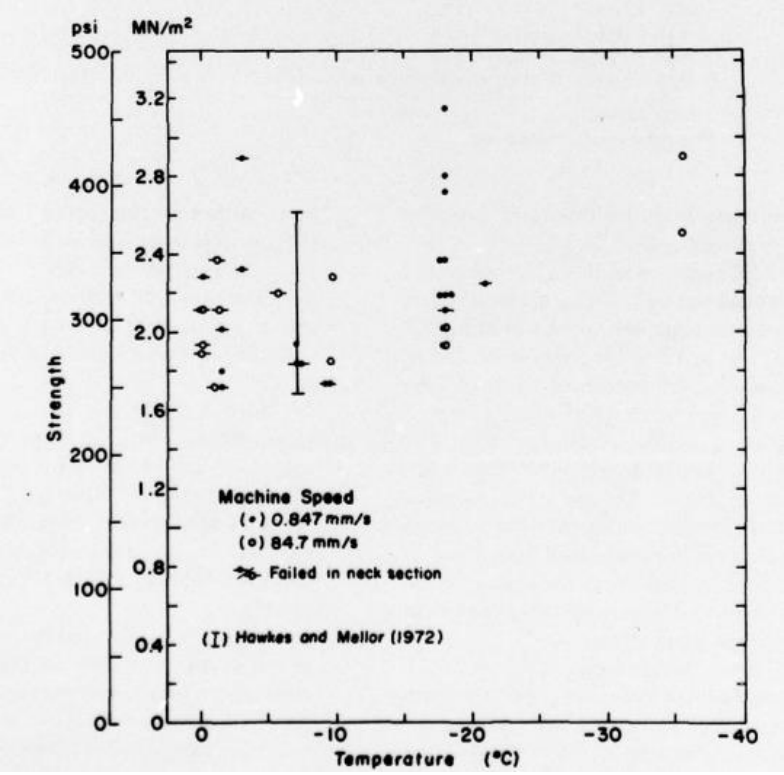

Figure 3-10 Ice tensile strength with temperature[18]

3.5 Selected material properties

The comprehensive material property is complex for this simulation. To simplify the simulation, tedious properties such as thermal property are neglected, and only the basic physical and mechanical properties are required. All the input data are listed from Table 3-4 to Table 3-6.

Table 3-4 Input steel material data

Density[kg/m3]	7850
Poisson's ration	0.3
Young's modulus[Ga]	210
Maximum plastic strain	0.267

Table 3-5 Strain VS stress of NV-A36[3]

Strain	Stress[Mpa]
0	0
0.0169	355 (yield strength)
0.045	370
0.1	440
0.2	520
0.3	565
0.4	598
0.5	621
0.6	640
0.7	660

Table 3-6 Input ice material data

	ice	rigid
Density[kg/m3]	900	2.00E+06
Poisson's ration	0.3	
Young's modulus[Ga]	210	
Maximum tensile pressure[Mpa]	7	

From Figure 3-9 and Figure 3-10, there is strength deviation of ice in a certain temperature. Hence, two relative higher values of ice strength will be used respectively.

[3] Only 10 stress strain pairs can be used in explicit dynamics systems.

4 Modelling Process

4.1 Geometry modelling

There are two objects in the simulation process: side hull structure of the container ship and the ice, showed in Figure 4-1. And the global coordinate is showed as well.

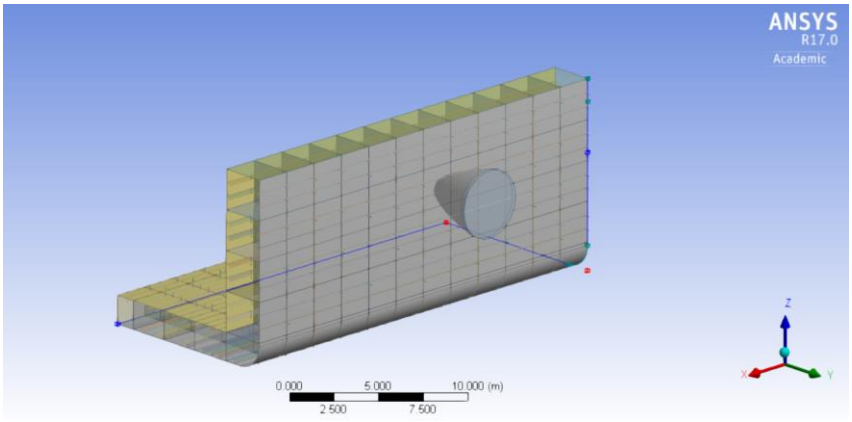

Figure 4-1 Geometry

4.1.1 Hull part

Only half of the hold needs to be built because of the symmetry. And some idealizations are made when modelling.

On the one hand, to save computation time, some unnecessary sub-structures such as transvers watertight bulkhead is neglected. To simulate the ignored part, corresponding boundary conditions are used.

On the other hand, to make the structure as continuous as possible, poly lines are used for sketching. For example, the inner side and inner bottom can be integrated when sketching. While the thickness can be changed respectively. In this way, not only can the model be more realistic, but also be much easier to extend.

The thickness of the plate and stiffener dimensions refers to Chapter 2. The main dimensions are listed in Table 4-1.

Table 4-1 Hull dimensions

Object	Value
Length [m]	25.5
Height from baseline[m]	11.36
Top width [m]	2.66
Hitting position from baseline[m]	8.54

The sub-structures also play important roles for the entire strength. There are 11 transvers side girders with the thickness of 15mm and 5 longitudinal floors (deck) with the thickness of 11mm to connect and support the inner side plate and outer side plate.

4.1.2 Ice part

The ice geometry consists of two parts: ice part and rigid body part. Real level ice or iceberg are large compared to the hull part. It is impossible to modelling the real shape and volume. To simplify the problem, a rigid body is used to replace the remote ice area which can provide necessary mass and kinetic energy but will not affect the collision results. It is worth mentioning that most mass of this geometry is from rigid body, around 3000ton, while the mass of ice is less than 50ton.

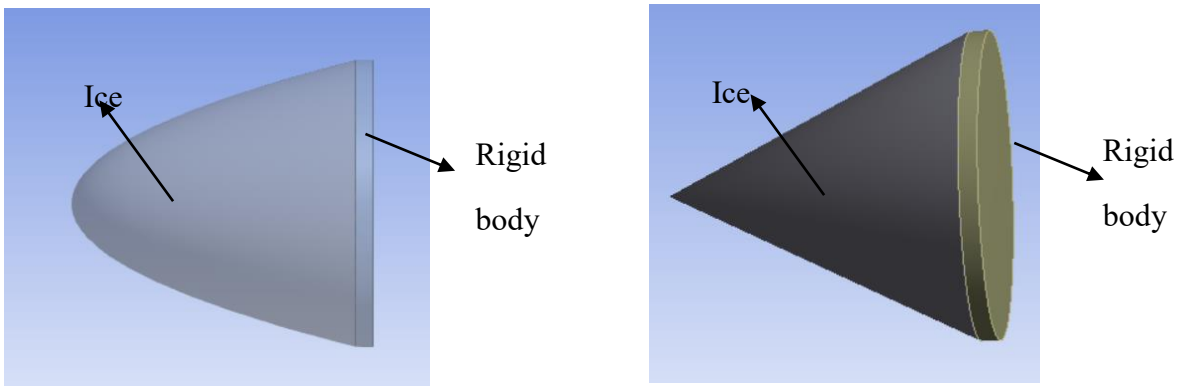

a. bullet ice b. cone ice

Figure 4-2 Ice geometry

4.2 Mesh

4.2.1 Mesh size

The strength of the hull part is of interest. While it is not wise to mesh all the hull part in small

size, for it will increase the computation time. Hence, only the collision part adopts small mesh size of 100mm. The mesh size of other parts of the hull is 500mm. The mesh size of ice is 300mm and of the rigid body is 500mm.

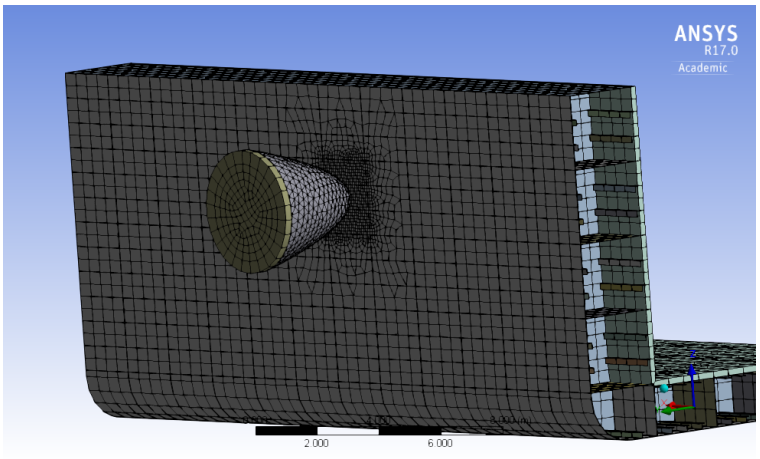

Figure 4-3 Mesh

4.3 Element type

4.3.1 Hull part

For the thin structure (the ration between thickness and other two dimensions is smaller than 1:5), shell element is recommended. In this simulation, Shell 181 is the default element type for the plate, girders and floors[12]. Shell 181 is well-suitable for thin structure with large rotation, deformation and non-linear applications. In other words, it is suitable for collisions simulations.

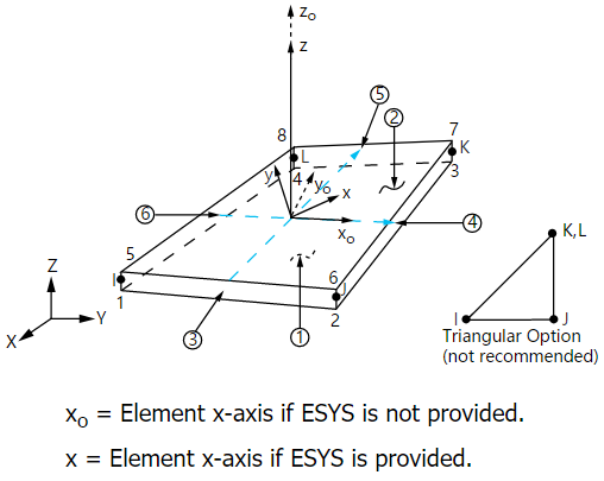

x_o = Element x-axis if ESYS is not provided.

x = Element x-axis if ESYS is provided.

Figure 4-4 Shell 181 illustration

4.3.2 Ice part

Solid 186 is the element type for ice. It is a higher order 3D 20-nodes solid element, which is defined by 20 nodes having three degrees of freedom per node: translations in the nodal x, y, and z directions49. The element supports plasticity, hyper-elasticity, creep, stress stiffening, large deflection, and large strain capabilities[12]. It is suitable for ice model.

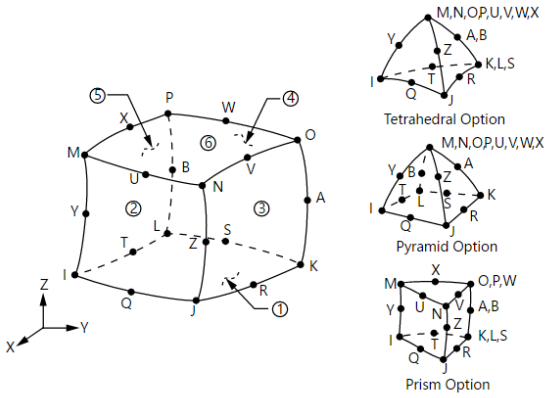

Figure 4-5 Solid 186 illustration

4.4 Initial and boundary conditions

Generally, for open water simulation. All the edges at both ends are fixed because they are connected to watertight bulkheads which are considered as rigid boundary. At the symmetry plane, the rotation is fixed while the vertical displacement is free.

The ice is assumed to be moving vertically to the hull structure, the displacement at global z direction in Figure 4-1 is fixed.

At first, the initial ice speed is assigned as -1.5m/s at only Y direction, with the distance of 0.01m between the hull and ice. The volume of rigid body will be changed with different ice shape to provide the same initial kinematic energy.

Table 4-2 Boundary conditions

	Displacement			Rotation		
	dx	dy	dz	Rx	Ry	Rz
Hull	fix	fix	fix	fix	fix	fix

(Continued Table 4-2)

	Displacement			Rotation		
	dx	dy	dz	Rx	Ry	Rz
Ice	free	free	fix	fix	fix	fix

4.5 Variables

There are 4 variables in the simulation: ice shape, hull scantling, hitting location and initial speed.

4.5.1 Ice shape

Ice shape will influence the collision results. Generally, the shaper the ice, the more serious the damage. 2 different ice shapes are modelled: bullet and cone.

a) bullet

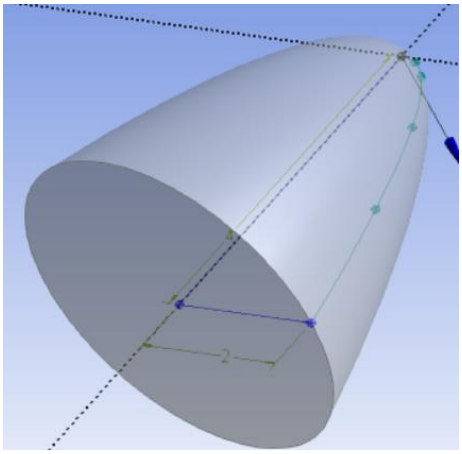

Figure 4-6 Bullet ice

The curve of the cross section is $y = x^2$ with a height of 4m and the bottom diameter of 4m.

b) cone

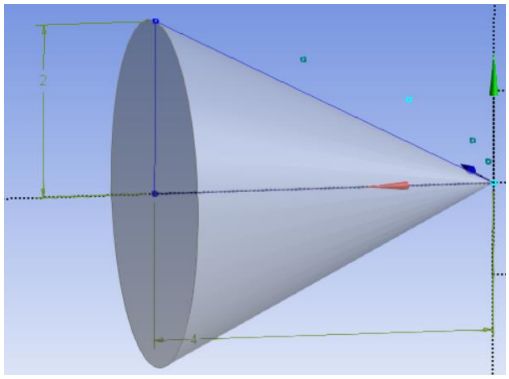

Figure 4-7 Cone ice

The height of the cone is 4m and the bottom diameter is 4m.

4.5.2 Hull dimensions

As discussed in Chapter 2, the results from different ice class rules were different. On the premise of the ship strength, less material does good to cost saving.

4.5.3 Hitting location

As illustrated in Chapter 3.1, to check the strength of different structure, several hitting positions of ice needs to be analysed. Two different positions are considered, one to check the strength of plate and longitudinal (the longitudinal spacing is small compared to the ice size, and it is not necessary to check the longitudinal strength respectively), and the other to check the strength of frame

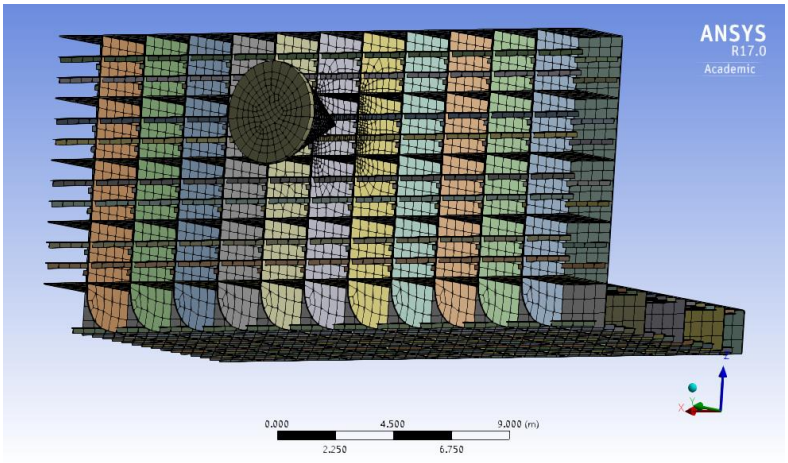

Figure 4-8 Hitting position on plate

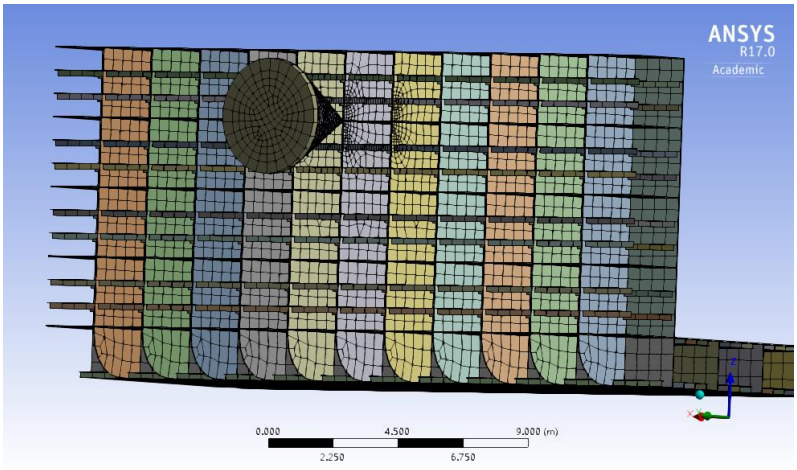

Figure 4-9 Hitting position on frame

4.5.4 Initial speed

Two cases of speed are discussed: with and without forward speed. Since the ship is fixed, to create a relative forward speed, the ice is assigned a speed in x direction. And another speed in y direction is assigned as vertical collision speed.

Table 4-3 Speed situations

	Ux[m/s]	Uy[m/s]	Uz[m/s]
With forward speed	10	-1.5	0
Without forward speed	0	-1.5	0

4.5.5 Ice scenario

Putting all the variables together, 12 typical scenarios in total are discussed. The results from one certain situation of the two class rules will be compared.

Table 4-4 Ice scenarios

Class rules	Ice Shape	Speed	Hitting position
IACS	Bullet Ice	Without forward speed	Hitting on the plate
			Hitting on frames
		With forward speed	
	Cone Ice	Without forward speed	Hitting on the plate
			Hitting on frames
		With forward speed	

(Continued Table 4-4)

Class rules	Ice Shape	Speed	Hitting position
FSICR	Bullet Ice	Without forward speed	Hitting on the plate
			Hitting on frames
		With forward speed	
	Cone Ice	Without forward speed	Hitting on the plate
			Hitting on frames
		With forward speed	

5 Results analysis

In the collision simulation, the damage area is of interest. The results would show the maximum strain, stress, and structural response of the selected scenarios and be compared in pairs, frame and plate area (definition in Chap. 4.5.3) respectively. The detailed FE analysis refers to A. APPENDIX.

5.1 Results summary

8 different scenarios were compared in pairs. The maximum equivalent stress and equivalent plastic strain were of interest. Both main plate and frame structure were checked in each scenario.

5.1.1 Bullet ice hitting on place area

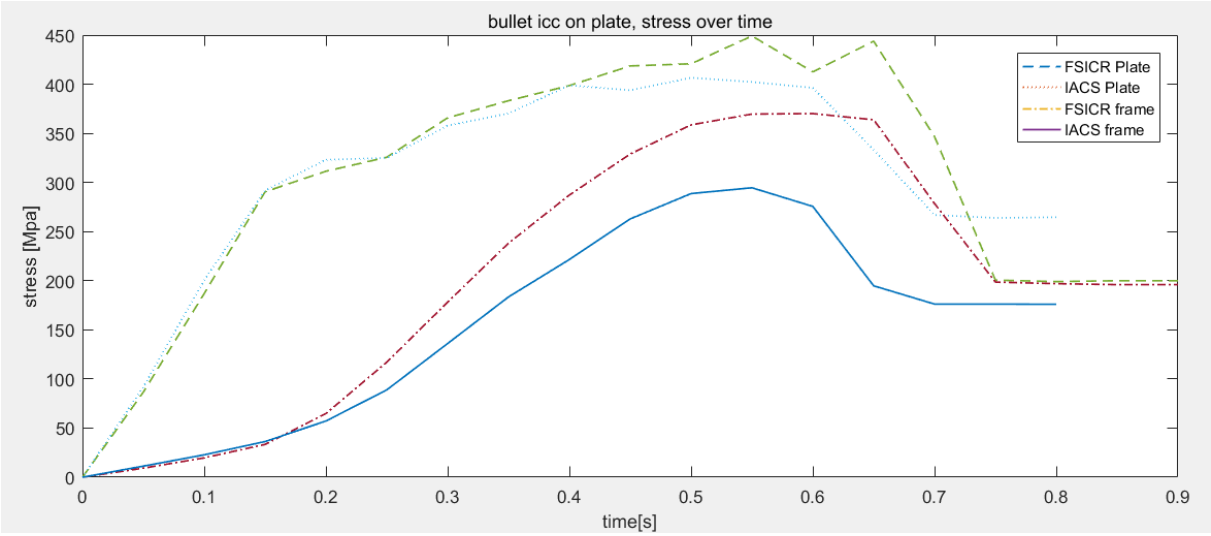

Figure 5-1 Maximum equivalent stress change over time for bullet ice hitting on plate area

Table 5-1 Solution of bullet ice hitting on plate

Ice class rule	IACS	FSICR
Maximum equivalent plastic strain on plate	0.216	0.245
Maximum equivalent plastic strain on frame	0.053	0.070
Maximum equivalent stress on plate[Mpa]	406.6	449.1
Maximum equivalent stress on frame[Mpa]	370.1	294.6

According to the results in Figure 5-1 and Table 5-1, the maximum stress took place on plate for both class rules. The maximum equivalent stress & strain from FSICR were higher than which from IACS PC. There was not any damage (failure area) for both situations, but the maximum equivalent plastic strain on plate of FSICR results was close to the failure criteria.

5.1.2 Cone ice hitting on place area

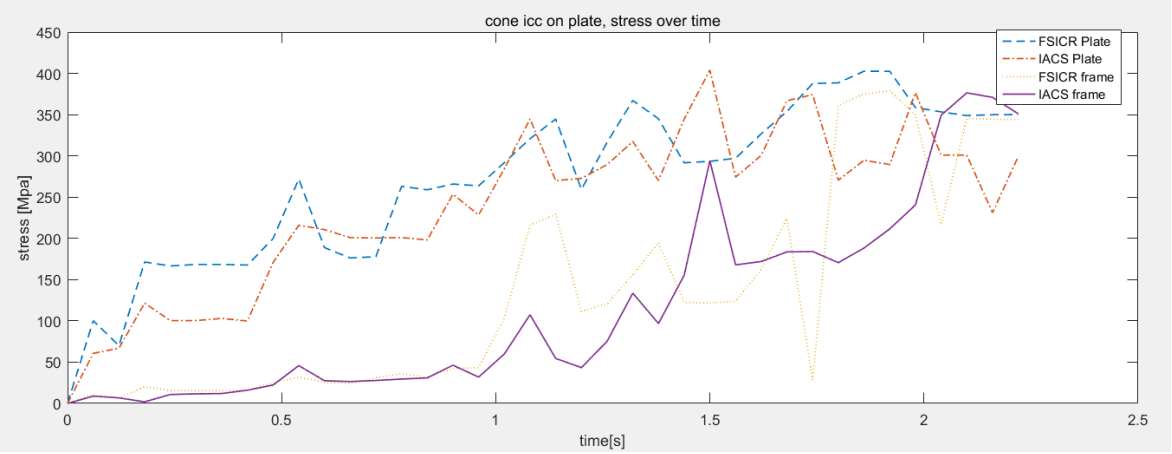

Figure 5-2 Maximum equivalent stress change over time for cone ice hitting on plate area

Table 5-2 Solution of cone ice hitting on plate

Ice class rule	IACS	FSICR
Maximum equivalent plastic strain on plate	0.189	0.180
Maximum equivalent plastic strain on frame	0.083	0.087
Maximum equivalent stress on plate[Mpa]	403.9	402.6
Maximum equivalent stress on frame[Mpa]	376.4	378.9

According to the results in Figure 5-2 and Table 5-2, the maximum stress took place on plate for both class rules. The maximum equivalent stress & strain from FSICR were close to which from IACS PC. There was not any damage (failure area) for both situations.

5.1.3 Bullet ice hitting frame area

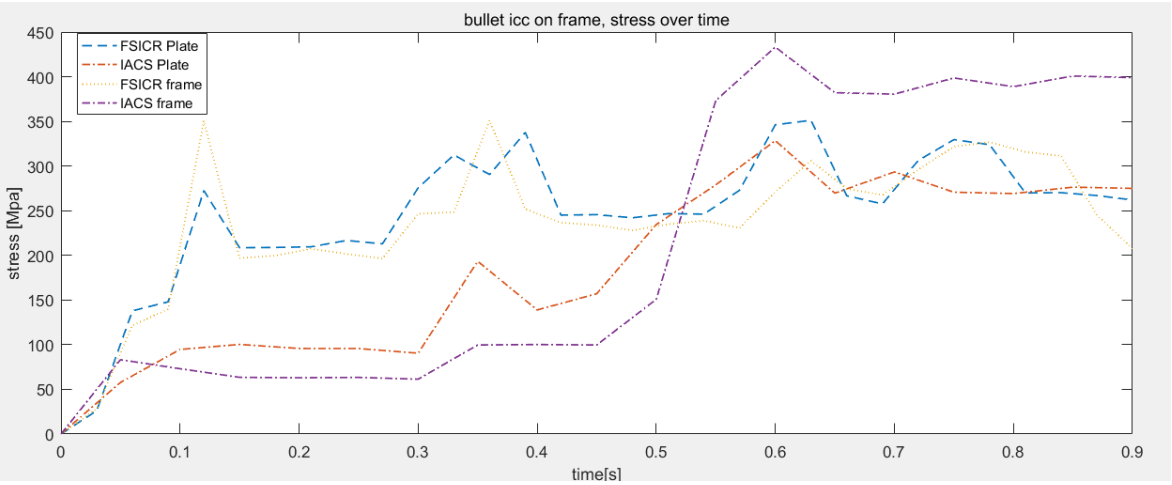

Figure 5-3 Maximum equivalent stress change over time for bullet ice hitting on frame area

Table 5-3 Solution of bullet ice hitting on frame

Ice class rule	IACS	FSICR
Maximum equivalent plastic strain on plate	0.155	0.089
Maximum equivalent plastic strain on frame	0.186	0.087
Maximum equivalent stress on plate[Mpa]	328.4	351.2
Maximum equivalent stress on frame[Mpa]	433.2	350.5

According to the results in Figure 5-3 and Table 5-3, the maximum stress took place on the frame for both class rules. The maximum equivalent strain from IACS were higher than which from FSICR PC. While the maximum equivalent stress on plate from IACS results was lower that which from FSICR. There was not any damage (failure area) for both situations.

5.1.4 Cone ice hitting on frame area

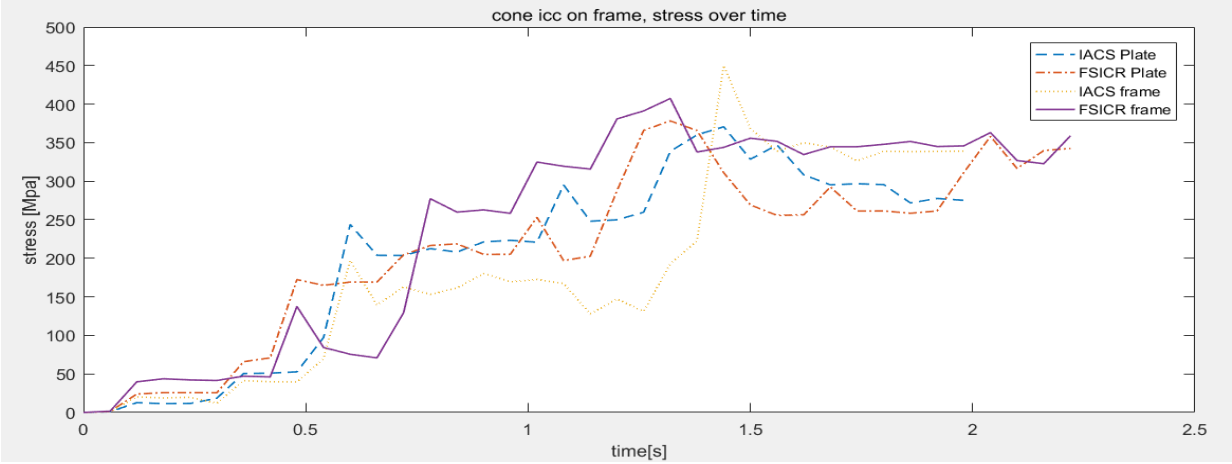

Figure 5-4 Maximum equivalent stress change over time for cone ice hitting on frame area

Table 5-4 Solution of cone ice hitting on frame

Ice class rule	IACS	FSICR
Maximum equivalent plastic strain on plate	0.136	0.191
Maximum equivalent plastic strain on frame	0.196	0.120
Maximum equivalent stress on plate[Mpa]	403.9	402.6
Maximum equivalent stress on frame[Mpa]	376.4	378.9

According to the results in Figure 5-4 and Table 5-4, the maximum stress took place on the frame for both class rules. The maximum stress from IACS were close to which from FSICR PC. There was not any damage (failure area) for both situations.

5.1.5 Bullet ice with forward speed

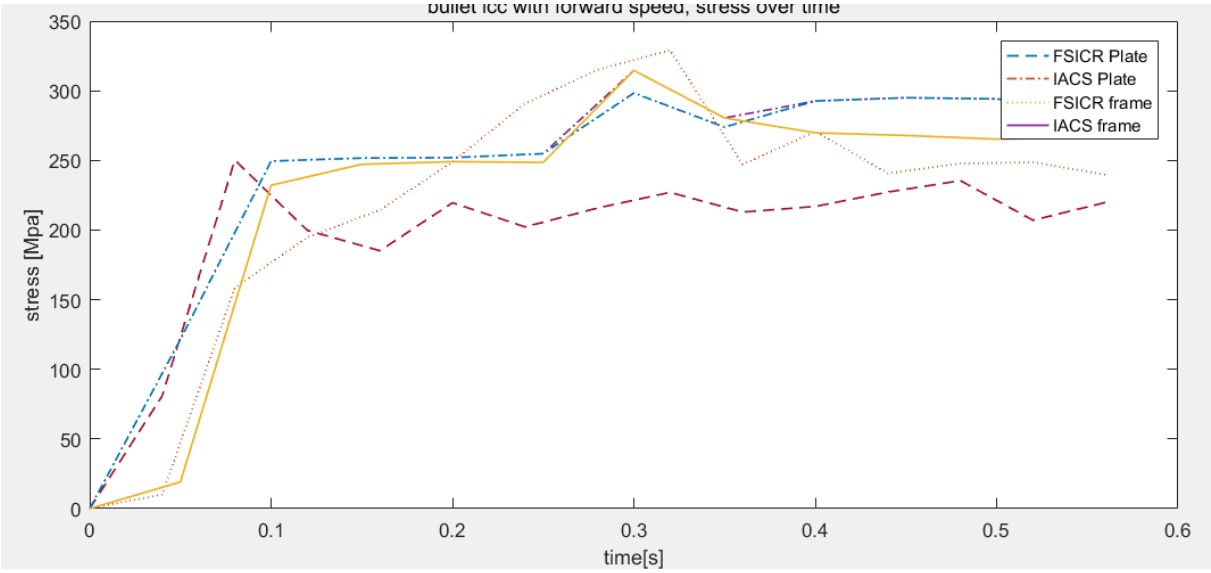

Figure 5-5 Maximum equivalent stress change over time for bullet ice with forward speed

Table 5-5 Solution of bullet ice with forward speed

Ice class rule	IACS	FSICR
Maximum equivalent plastic strain on plate	0.059	0.049
Maximum equivalent plastic strain on frame	0.087	0.056
Maximum equivalent stress on plate[Mpa]	298.4	250.2
Maximum equivalent stress on frame[Mpa]	314.5	329.9

According to the results in Figure 5-5 and Table 5-5, the maximum stress took place on the frame for both class rules. The maximum stress from IACS were close to which from FSICR PC. There was not any damage (failure area) for both situations.

5.1.6 Cone ice with forward speed

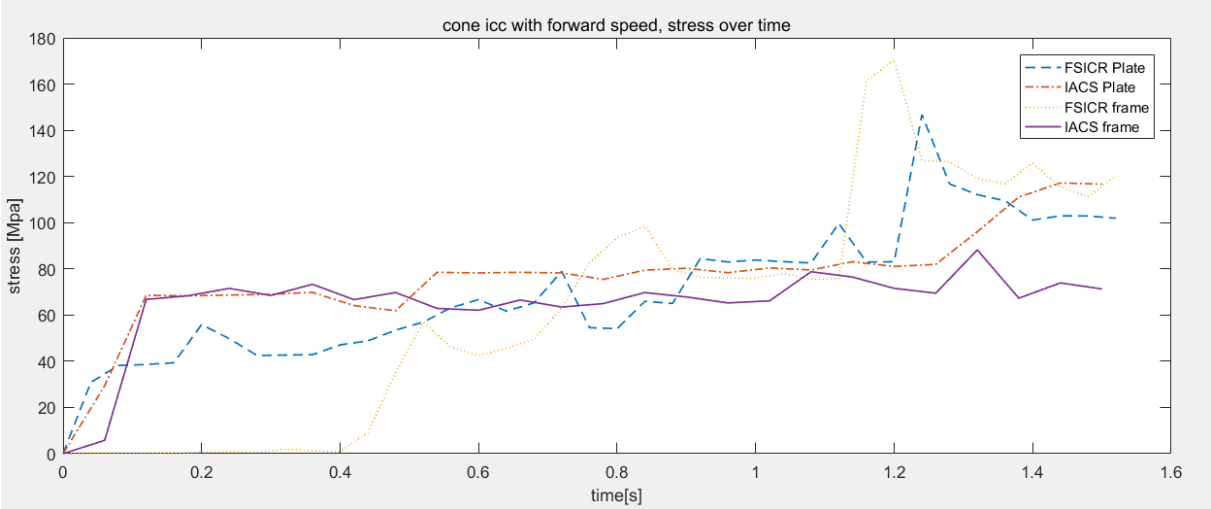

Figure 5-6 Maximum equivalent stress change over time for cone ice with forward speed

Table 5-6 Solution of cone ice with forward speed

Ice class rule	IACS	FSICR
Maximum equivalent plastic strain on plate	0.024	0.034
Maximum equivalent plastic strain on frame	0.028	0.030
Maximum equivalent stress on plate[Mpa]	119.6	146.7
Maximum equivalent stress on frame[Mpa]	88.2	170.1

According to the results in Figure 5-6 and Table 5-6, the maximum stress took place on the frame for both class rules. The maximum stress from IACS were a little lower than which from FSICR PC. There was not any damage (failure area) for both situations.

5.2 Comparison & analysis of the results

The results in the first group (APPENDIX A.1 case i to iv) were quite similar. There was permanent deformation on both the hull structures. The maximum strain was on the plate, as well as the deformation. This results were predictable. Meanwhile, the frames also had obvious deformation, and the deformation on the floors was more critical than girders. For the thickness of floors from both designs were thinner that girders. The load acting on frames were like press load in axial direction, and it started buckling, which would be potential hazards to second impacts.

For the second group (APPENDIX A.2 case v to viii), though the form of results from were similar, the value differed significantly. Generally, the maximum strain was expected occurred on the frames, or the maximum strain on the plate and the frame was close to each other. While the case vii was an exception. For this case, the maximum strain on the plate was double of the strain on the frame. It could not say that the results were wrong. During the hitting process, the ice was crashed all the time. The critical contact point could change randomly as well as the location of maximum stress (figure 5-5). Hence, the situation in case vii could happen.

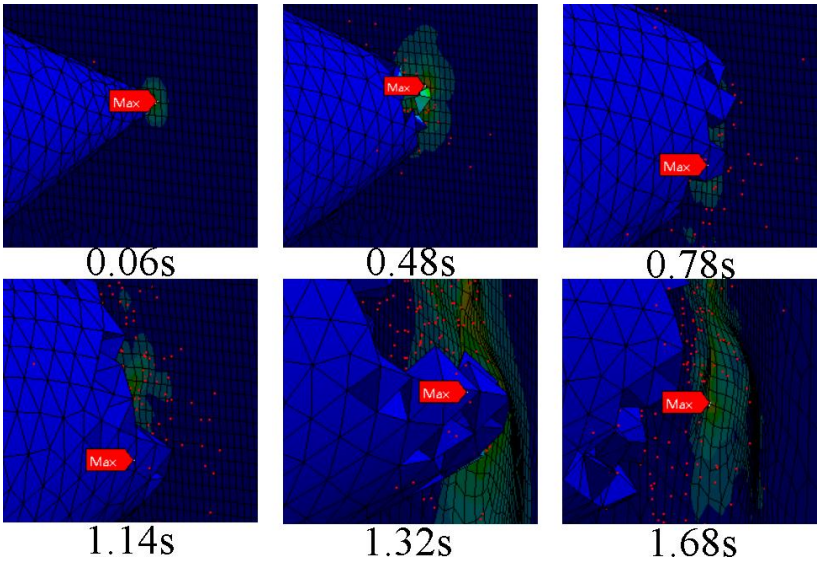

Figure 5-7 Location of maximum stress changes over time

As for the value, they were far from excepted. The maximum strain from FSICR were almost half of IACS (case v & vi, vii & viii, or from Table 5-3 and Table 5-4). While the scantling of FSICR design was smaller than IACS design. In other words, to design degree, the IACS design

should be stronger than FSICR design.

Then, for the last group (APPENDIX A.3, case ix to xii) with forward speed. Though the plastic deformation area was larger than the former cases. The value of deformation or strain was so small that could be neglected. Besides, the results from two class rules were close to each other.

6 Conclusion

The Finnish-Swedish Ice Class Rules (FSICR) has a long history. Having being tested by countless ships, it becomes the authority in Baltic Sea region. International Association of Classification Societies Polar Class (IACS PC) is first published in 2007, and it unifies other rules together.

In this thesis, all the scenarios are within safety range. FSICR design with fewer materials are more competitive than IACS design.

According to definition of ice class, for level ice, IACS PC 7 are equivalent to FSICR IA and should be higher than FSICR IC. It is true at the design stage. The scantling from IACS PC7 design are larger than FSICR IC design, but not too much. As a result, the strength from IACS design is supposed to be higher than FSICR design.

However, according to the results above, the situation was a little different for iceberg scenario. For case v to viii, the results opposites the expectation. The FSICR design showed the same or even higher strength than IACS design. The randomness of the ice crashing process was the main reason. For example, the crash of ice might create new sharp points (Figure 5-7), which would cause secondary damage in a single collision process.

The ice state changes all the time. In Baltic Sea, there are not only level ice in winters, but also ice ridges. A vessel may endanger more than once collisions in an area with high density of ice ridges or icebergs. The large plastic deformation from the first-time collision definitely can be a hazard to the vessel.

In the collision process, the initial kinematic energy of ice transfers to internal energy of structure (plastic deformation and damage), friction energy, crashing energy of ice and the left kinematic energy of ice.

To avoid damage or large plastic deformation, some measures can be taken. Vessel displacement, engine output, materials, and frame arrangement are the main factors in the design process for both rules. Apart from them, some rule-defined factors also influence the designs. for example, the crashing failure factor in IACS PC and the height of load area in FSICR. Although the

design process is rigid, some variables above can be changed for both ice class rules. At the design stage, on the one hand, the number of stiffeners can be increased within the ice belt. On the other hand, the frame spacing can be decreased. These two methods are claimed in many ice rules. However, the potential stress concentration need to be considered. Moreover, a stronger material can be used. But the cost is to be rise substantially.

The safety and cost are the two major considerations. To save cost as much as possible, the selection of rules is supposed to relate with the ice state, and with or without escort. FSICR is intended for only first-year level ice, and the grading classification is less in numbers but more precise compared with IACS PC. Combined with the simulation results, FSICR is more suitable for designing ships sailing in Baltic Sea.

7 Future work

Though, many works have been done in the thesis, and More works can be improved in the future work.

A better ice model

As discussed in the thesis, the ice property changes with environment. And ice is not a simple elastic and brittle material. Its strength is related with the strain rate and it has some plastic features. It is too difficult to apply exact data it in the simulation. While different ice properties can be used in the future work.

Steel material property

The collision failure is supposed to connect with the strain rate. The strain & stress will have variance for the same material. For example, the strain & stress rate is different under different temperature. And the failure criteria will decrease with a higher strain rate.

Moreover, the maximum equivalent plastic strain is calculated based on a fitting formula. To get a more accurate value, more material test should be carried out.

More variables can be considered

There are 4 variables in the thesis already. But the number of each is few. More numbers of variables can be considered e.g. the collision speed can be 2m/s and 3m/s, more ice shapes can be modelled. The computation of each scenario is time consuming. It is not possible to do all the potential cases, but can do as much as possible.

Full-scale collision experiment

All the simulation should be based on experiment. It is possible to carry out model experiments. Full-scale experiment for ice-ship collision is too expensive to do. But it is required to better the simulation results.

Reference

[1]. International Maritime Association. (2011). *International Shipping Facts and Figures–Information Resources on Trade, Safety, Security, and the Environment.* London: International Maritime Association.

[2]. Philipp S. (2015): *Initial Ship Design 800 TEU Container Ship Report*. KTH Royal Institute of Technology. Sweden.

[3]. Jinchao Z.&Yixiang S. (2015): *Marine Structure Project Hull Structure Design Report.* KTH Royal Institute of Technology. Sweden.

[4]. Veritas, D. N. (2009). *Hull structural design ships with length 100 meters and above.* Rules for Classification of SHIPS. Part 3, Chapter 1.

[5]. Riska, K., & Kämäräinen, J. (2011, November). *A review of ice loading and the evolution of the finnish-swedish ice class rules.* In Proceedings of the SNAME Annual Meeting and Expo. (pp. 16-18).

[6]. Choi, K. S., & Jeong, S. Y. (2008). *Ice load prediction formulas for icebreaking cargo vessels.* Journal of the Society of Naval Architects of Korea, 45(2), 175-185.

[7]. Kämäräinen, J., & Riska, K. *Ice Class Rules and International Regulations*. Encyclopedia of Maritime and Offshore Engineering.

[8]. International Association of Classification Societies (IACS) (2011). *Requirements Concerning POLAR CLASS*.

[9]. Finnish Transport Safety Agency (TraFi) (2010) *The Structural Design and Engine Output Required of Ships for Navigation In Ice "Finish-Swedish Ice Class Rules".*

[10]. Qi Kui-li. Liu J. (2014, June): *Strength Assessment of Polar Ships under Ice Loads Using Direct Calculation Method*. Journal of Ship Mechanics, 18(6), 1007-7294.

[11]. Bae, D. M., Prabowo, A. R., Cao, B., Sohn, J. M., Zakki, A. F., & Wang, Q. (2016). *Numerical Simulation for the Collision Between Side Structure and Level Ice in Event of Side Impact Scenario.* Latin American Journal of Solids and Structures, 13(16), 2991-3004.

[12]. Daley, C. G. (1999, August). *Energy based ice collision forces.* In Proceedings of the 15th

International Conference on Port and Ocean Engineering under Arctic Conditions, Helsinki University of Technology in Espoo, Finland.

[13]. ANSYS, Inc. (2016). *ANSYS 17.0 Help Viewer*. Available at: https://www.sharcnet.ca/Software/Ansys/17.0 (accessed on 8 April 2017).

[14]. Veritas, D. N. (2015, January): *Ships for Navigation in Ice.* Rules for Classification of Ships, Part 5, Chapter 1.

[15]. Lyngra, N. H. L. (2014). *Analysis of Ice-Induced Damages to a Cargo Carrier and Implications wrt. Rule Requirements* (Master's thesis, Institutt for marin teknikk).

[16]. Veritas, D. N. (2013 June). *Determination of Structural Capacity by Non-linear FE analysis Methods*. Recommendation Practice, DNV-RP-C208.

[17]. Liu, Z., Amdahl, J., & Løset, S. (2011). *Plasticity based material modelling of ice and its application to ship–iceberg impacts*. Cold regions science and technology, 65(3), 326-334.

[18]. Haynes, F. D. (1978). *Effect of temperature on the strength of snow-ice* (No. CRREL-78-27). COLD REGIONS RESEARCH AND ENGINEERING LAB HANOVER NH.

[19]. Ehlers, S., & Østby, E. (2012). *Increased crashworthiness due to arctic conditions–The influence of sub-zero temperature*. Marine Structures, 28(1), 86-100.

A. APPENDIX FEA Solution

The results can be divided two groups: plate area without forward speed, frame area without forward speed and with forward speed.

A.1 Without forward speed, plate area

i) FSICR design, bullet ice hitting on plate area

The ice started hitting the hull at an initial speed of 1.5m/s, and bounced at the speed of 0.38m/s. The maximum stress exceeded the yield strength, and the structure entered the plastic deformation. The maximum equivalent plastic stress was 0.245 on the plate, happening, on the plate, under the failure criteria, and no damage occurred in the process.

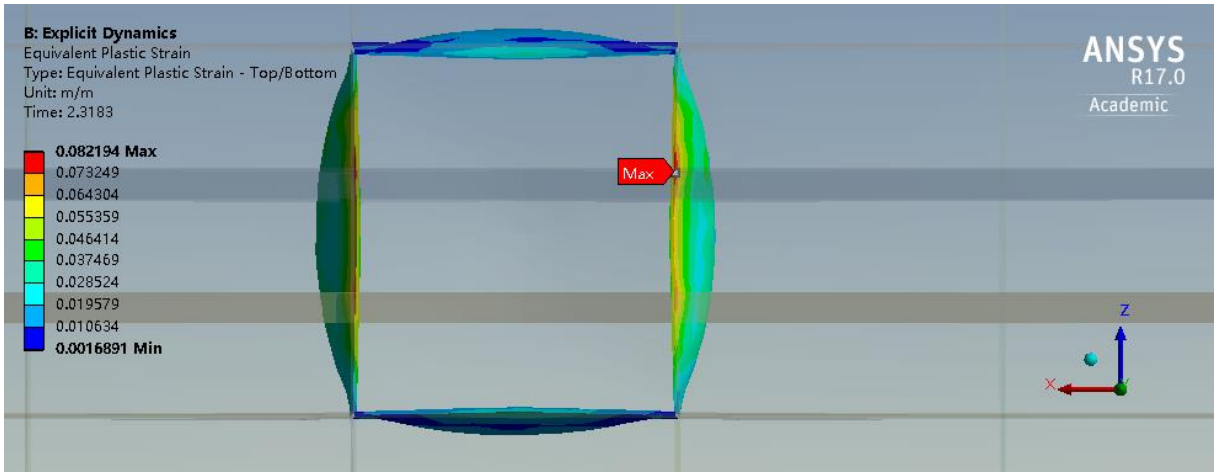

a. frame strain distribution

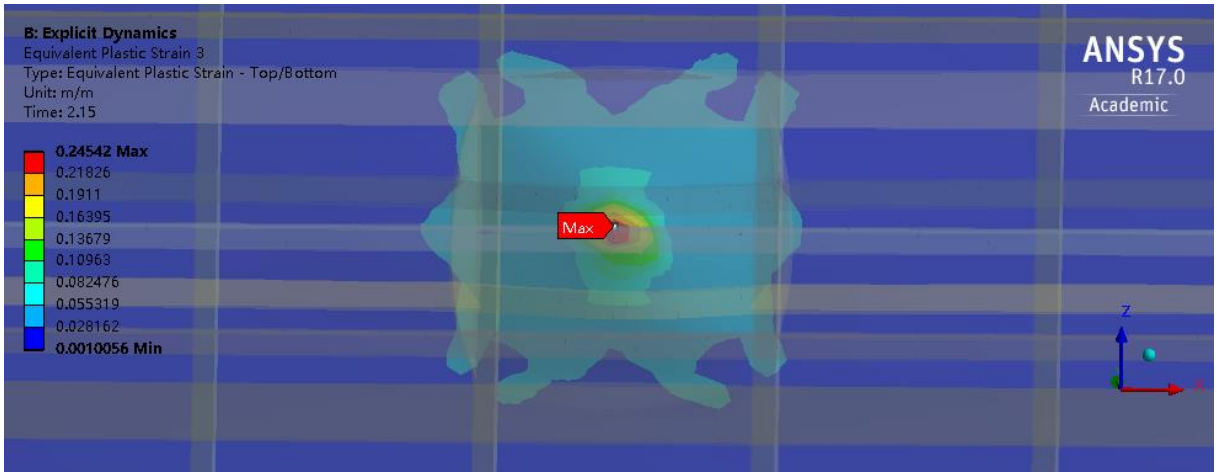

b. plate strain distribution

Figure A-1 Final equivalent plastic strain distribution of FSICR design, bullet ice, plate area

Table A-1 Simulation results of FSICR design, bullet ice, plate area

Object	value
Ice initial speed[m/s]	1.5
Bounced speed[m/s]	0.38
Ice mass[t]	3169
Kinetic energy loss[J]	3336323
Damage area on plate[m^2]	0
Damage area on frame[m^2]	0
Maximum deformation on plate[m]	0.67
Maximum deformation on frame[m]	0.263
Computation time[min]	498

ii) IACS design, bullet ice hitting on plate area

The ice started hitting the hull at an initial speed of 1.5m/s, and bounced at the speed of 0.41m/s. The maximum stress exceeded the yield strength, and the structure entered the plastic deformation. The maximum equivalent plastic stress was 0.216, happening on the plate, under the failure criteria, and no damage occurred in the process.

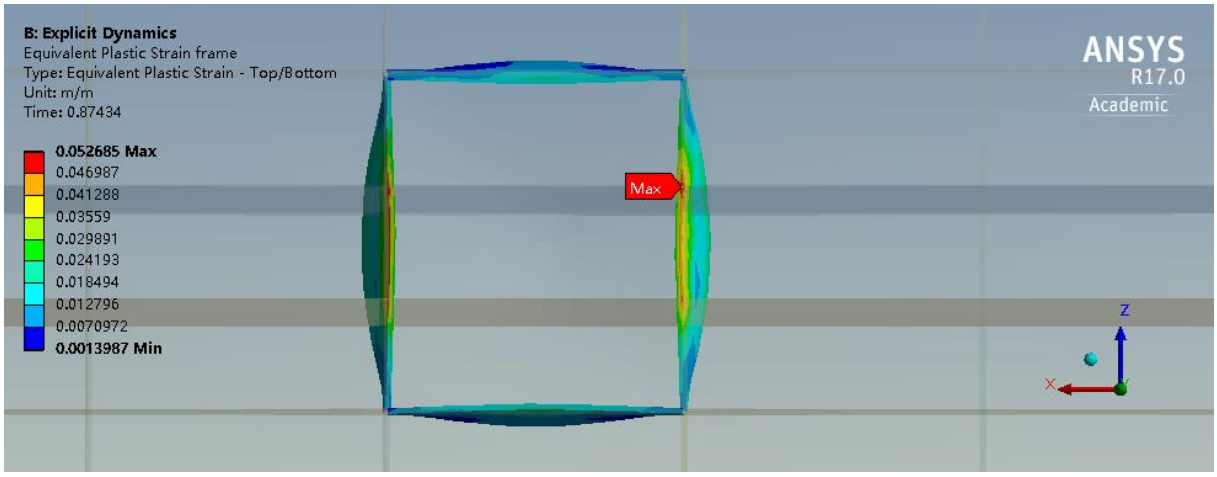

a. frame strain distribution

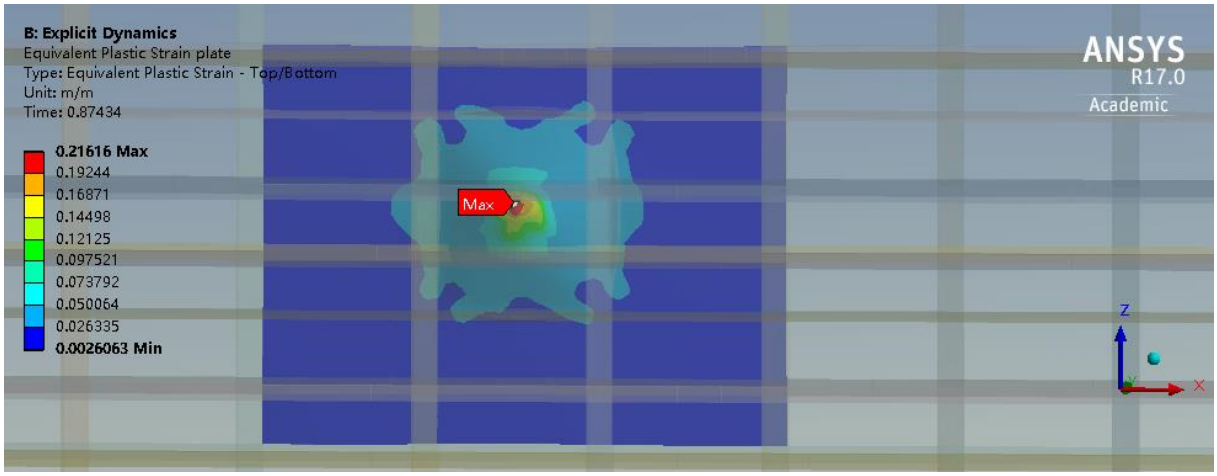

b. frame strain distribution

Figure A-2 Final equivalent plastic strain distribution of IACS design, bullet ice, plate area

Table A-2 Simulation results of FSICR design, cone ice, frame area

Object	value
Ice initial speed[m/s]	1.5
Bounced speed[m/s]	0.69
Ice mass[t]	3169

(Continued Table A-2)

Object	value
Kinetic energy loss[J]	2819939
Damage area on plate[m^2]	0
Damage area on frame[m^2]	0
Maximum deformation on plate[m]	0.253
Maximum deformation on frame[m]	0.156
Computation time[min]	434

iii) FSICR design, cone ice hitting on plate area

The ice started hitting the hull at an initial speed of 1.5m/s, and bounced at the speed of 0.57m/s. The maximum stress exceeded the yield strength, and the structure entered the plastic deformation. The maximum equivalent plastic stress was 0.18, happening on the plate under the failure criteria, and no damage occurred in the process.

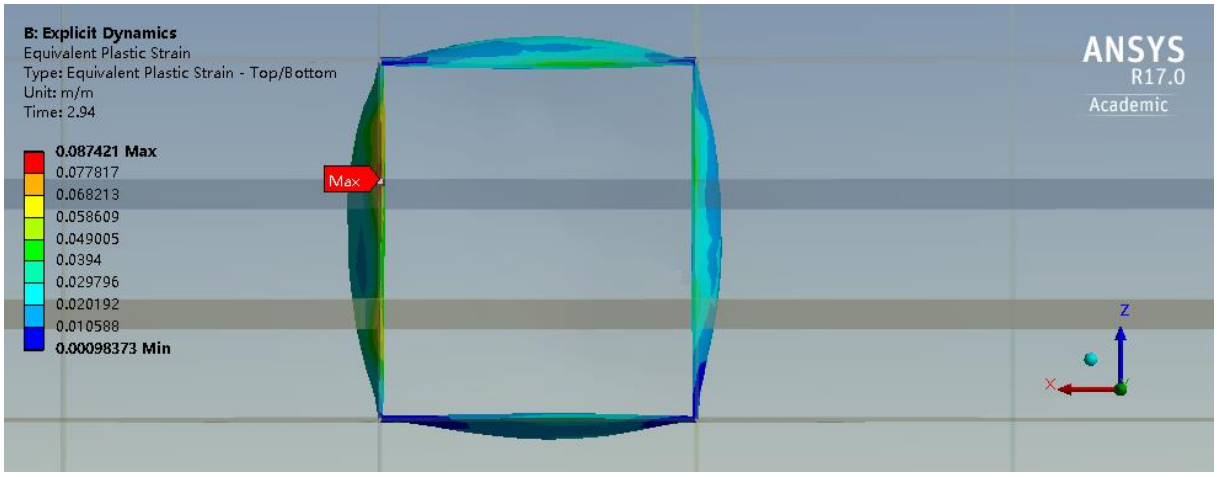

a. frame strain distribution

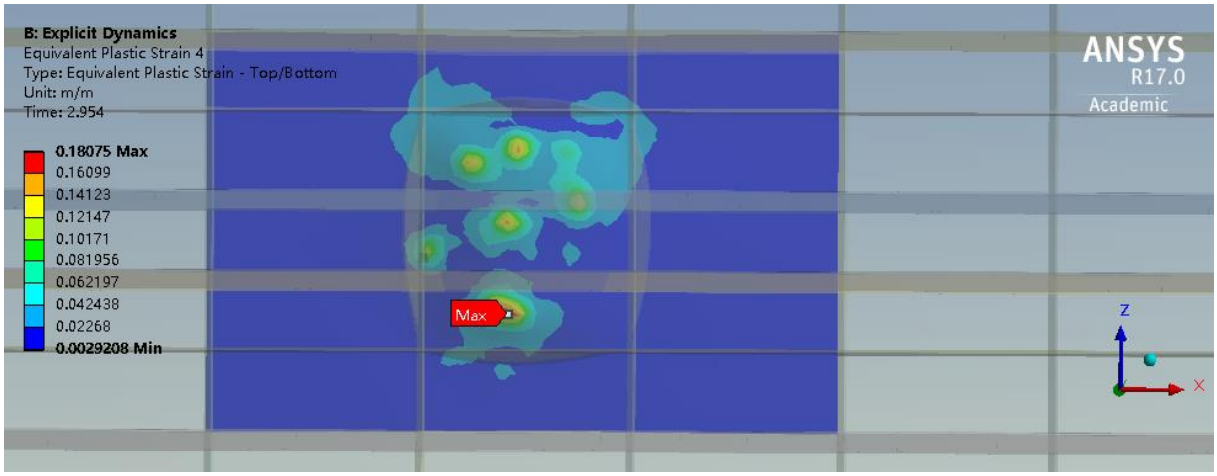

b. plate strain distribution

Figure A-3 Final equivalent plastic strain distribution of FSICR design, cone ice, plate area

Table A-3 Simulation results of FSICR design, cone ice, plate area

Object	value
Ice initial speed[m/s]	1.5
Bounced speed[m/s]	0.57
Ice mass[t]	3155

(Continued Table A-3)

Object	value
Kinetic energy loss[J]	3036845
Damage area on plate[m^2]	0
Damage area on frame[m^2]	0
Maximum deformation on plate[m]	0.434
Maximum deformation on frame[m]	0.227
Computation time[min]	403

vi) IACS design, cone ice hitting on plate area

The ice started hitting the hull at an initial speed of 1.5m/s, and bounced at the speed of 0.82m/s. The maximum stress exceeded the yield strength, and the structure entered the plastic deformation. The maximum equivalent plastic stress was 0.189, happening on the plate, under the failure criteria, and no damage occurred in the process.

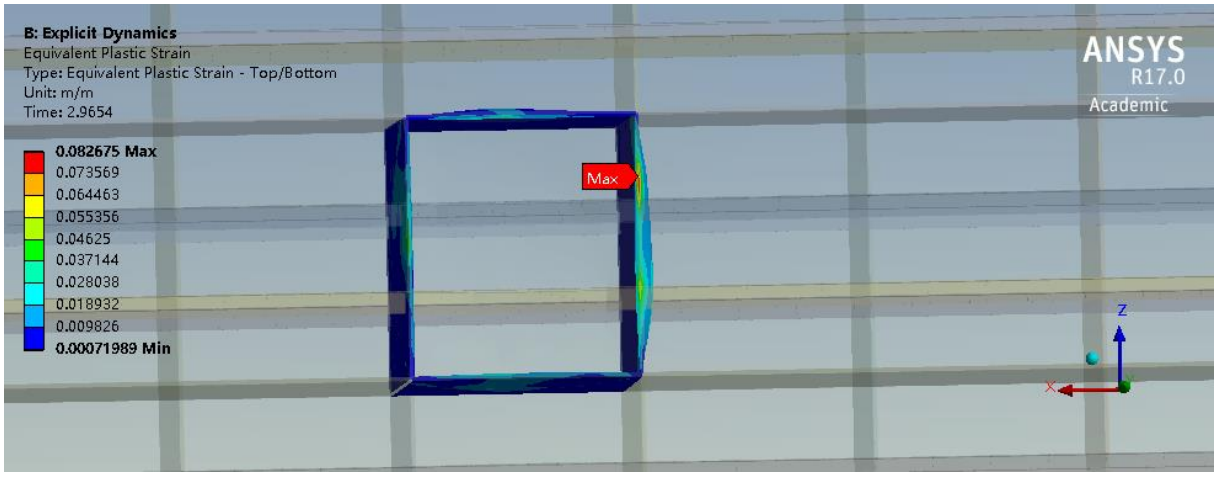

a. frame strain distribution

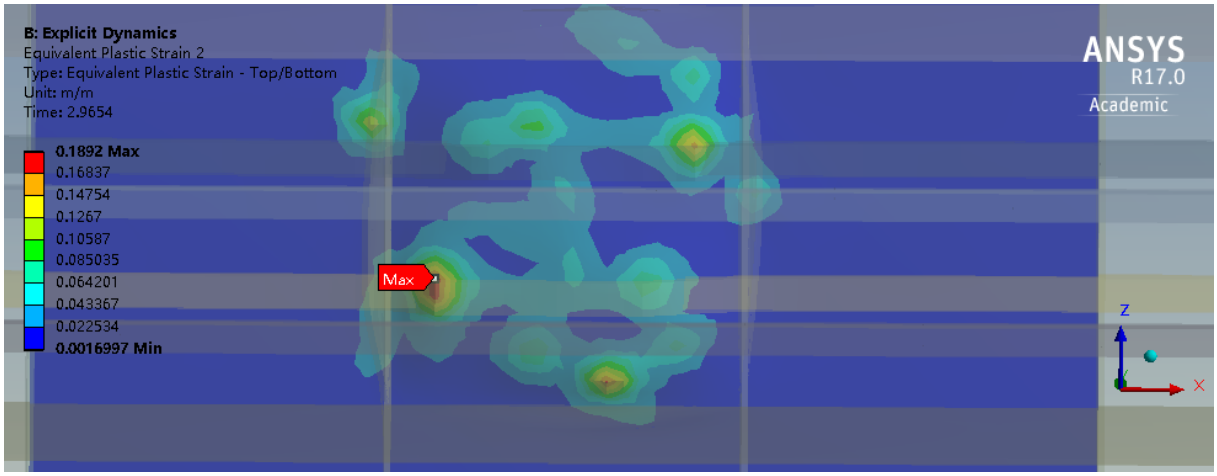

b. plate strain distribution

Figure A-4 Final equivalent plastic strain distribution of IACS design, cone ice, plate area

Table A-4 Simulation results of IACS design, cone ice, plate area

Object	value
Ice initial speed[m/s]	1.5
Bounced speed[m/s]	0.82
Ice mass[t]	3155

(Continued Table A-4)

Object	value
Kinetic energy loss[J]	2488664
Damage area on plate[m^2]	0
Damage area on frame[m^2]	0
Maximum deformation on plate[m]	0.301
Maximum deformation on frame[m]	0.144
Computation time[min]	475

A.2 Without forward speed, frame area

v) FSICR design, bullet ice hitting on frame area

The ice started hitting the hull at an initial speed of 1.5m/s, and bounced at the speed of 0.32m/s. The maximum stress exceeded the yield strength, and the structure entered the plastic deformation. The maximum equivalent plastic stress was 0.09, happening on the frame, under the failure criteria, and no damage occurred in the process.

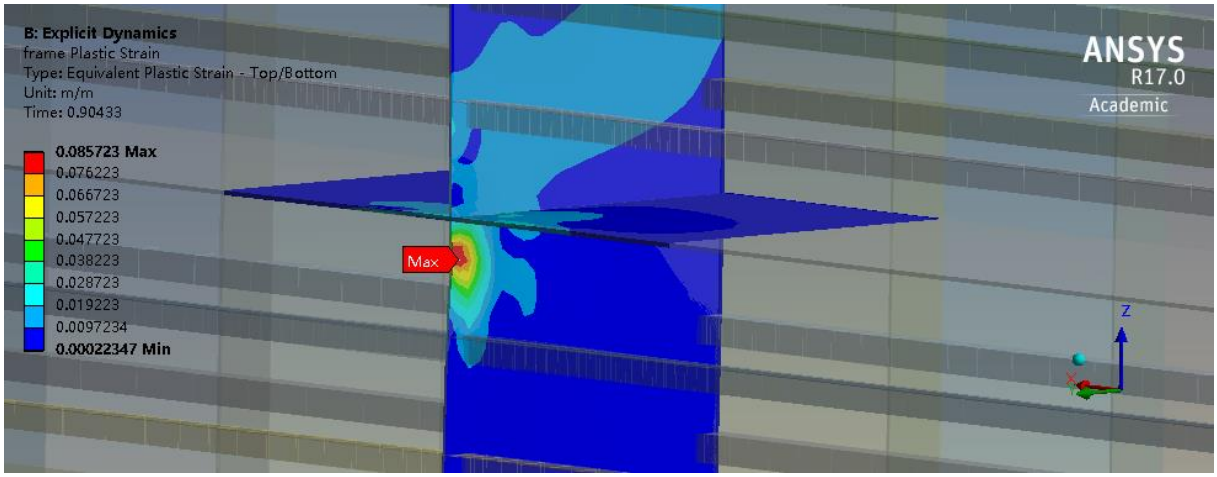

a. frame strain distribution

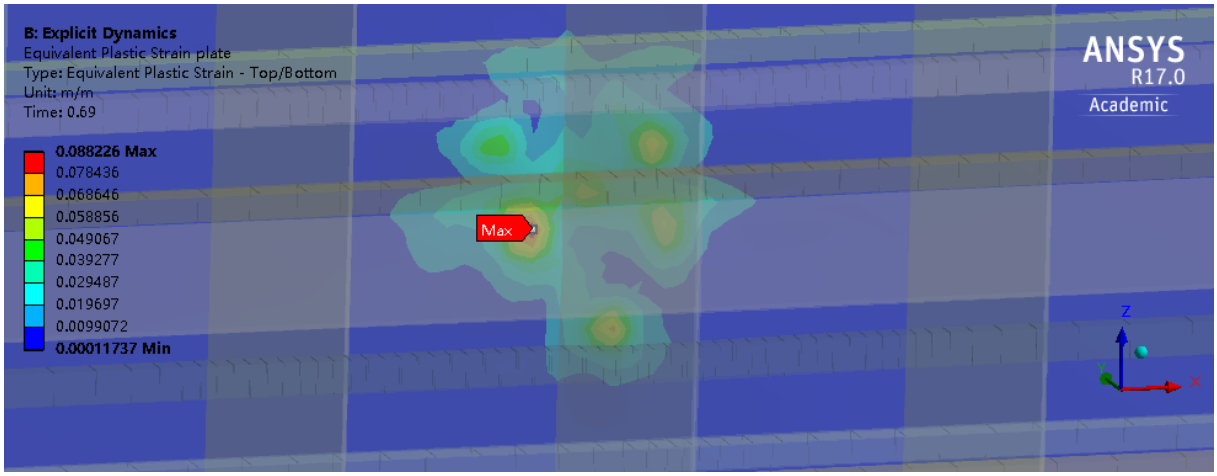

b. plate strain distribution

Figure A-5 Final equivalent plastic strain distribution of FSICR design, bullet ice, frame area

Table A-5 Simulation results of FSICR design, bullet ice, frame area

Object	value
Ice initial speed[m/s]	1.5

(Continued Table A-5)

Object	value
Bounced speed[m/s]	0.32
Ice mass[t]	3169
Kinetic energy loss[J]	3402872
Damage area on plate[m^2]	0
Damage area on frame[m^2]	0
Maximum deformation on plate[m]	0.169
Maximum deformation on frame[m]	0.082
Computation time[min]	862

vi) IACS design, bullet ice hitting on frame area

The ice started hitting the hull at an initial speed of 1.5m/s, and bounced at the speed of 0.71m/s. The maximum stress exceeded the yield strength, and the structure entered the plastic deformation. The maximum equivalent plastic stress was 0.186, happening on the frame, under the failure criteria, and no damage occurred in the process.

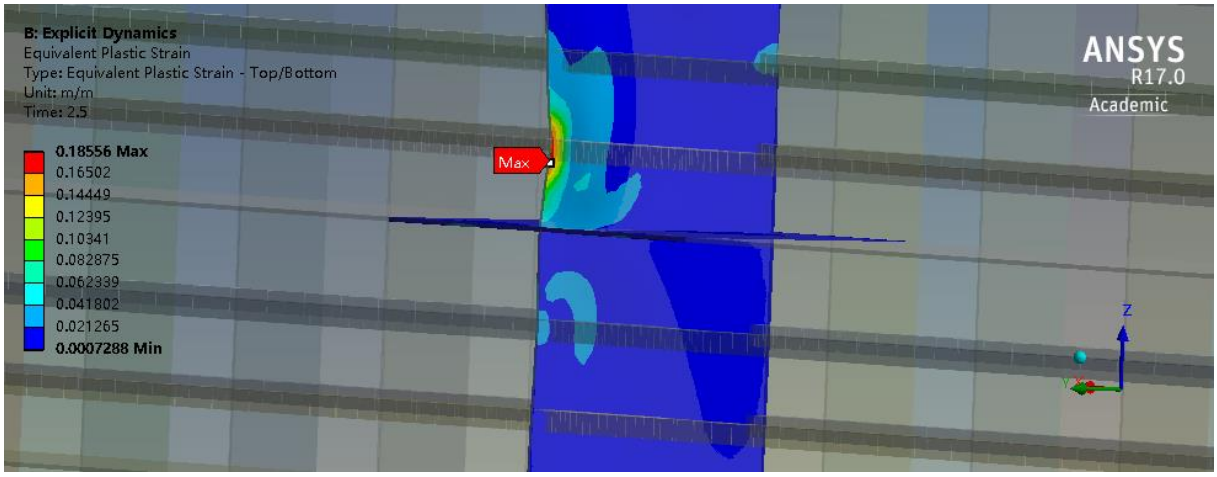

a. frame strain distribution

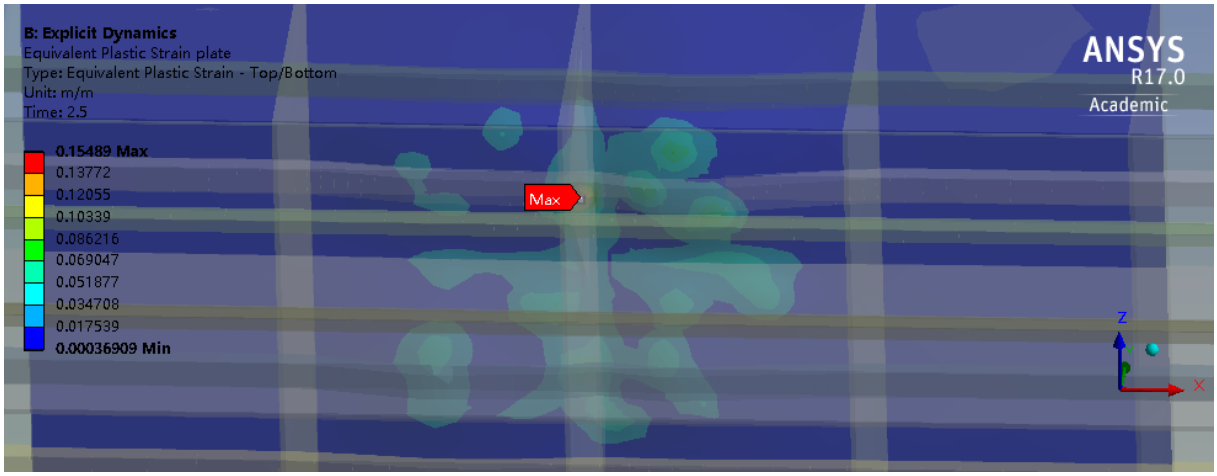

b. frame strain distribution

Figure A-6 Final equivalent plastic strain distribution of IACS design, bullet ice, frame area

Table A-6 Simulation results of IACS design, bullet ice, frame area

Object	value
Ice initial speed[m/s]	1.5
Bounced speed[m/s]	0.71
Ice mass[t]	3169

(Continued Table A-6)

Object	value
Kinetic energy loss[J]	2766379
Damage area on plate[m^2]	0
Damage area on frame[m^2]	0
Maximum deformation on plate[m]	0.226
Maximum deformation on frame[m]	0.172
Computation time[min]	820

vii) FSICR design, cone ice hitting on frame area

The ice started hitting the hull at an initial speed of 1.5m/s, and bounced at the speed of 0.69m/s. The maximum stress exceeded the yield strength, and the structure entered the plastic deformation. The maximum equivalent plastic stress was 0.191, happening on the plate, under the failure criteria, and no damage occurred in the process.

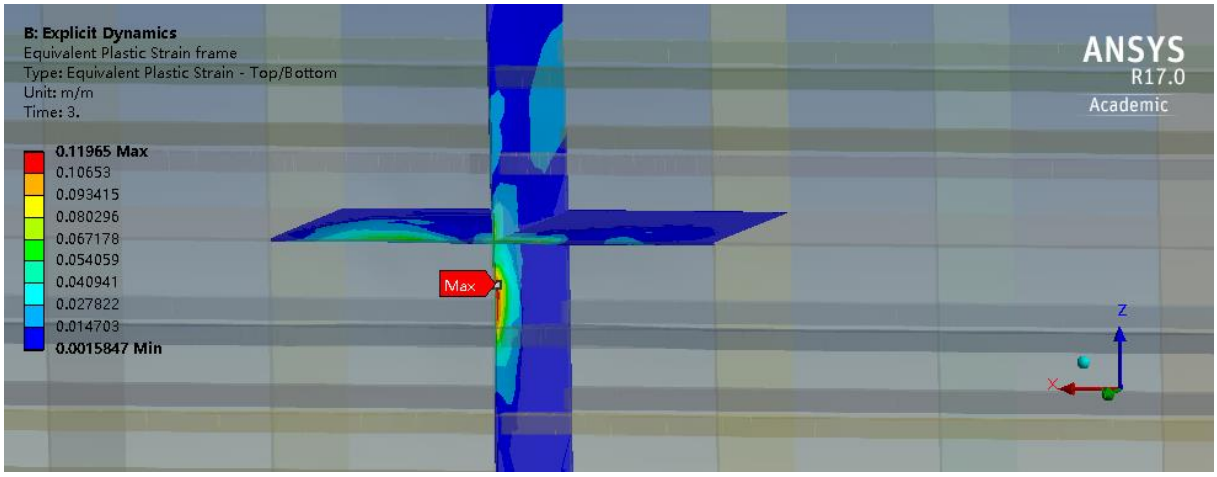

a. frame strain distribution

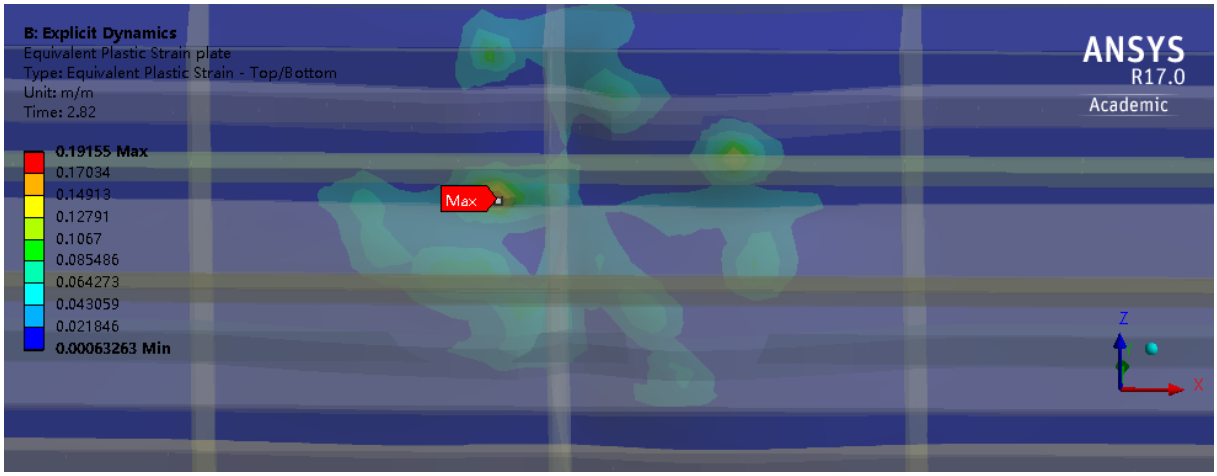

b. frame strain distribution

Figure A-7 Final equivalent plastic strain distribution of FSICR design, cone ice, frame area

Table A-7 Simulation results of FSICR design, cone ice, frame area

Object	value
Ice initial speed[m/s]	1.5
Bounced speed[m/s]	0.69
Ice mass[t]	3155

(Continued Table A-7)

Object	value
Kinetic energy loss[J]	2819939
Damage area on plate[m^2]	0
Damage area on frame[m^2]	0
Maximum deformation on plate[m]	0.253
Maximum deformation on frame[m]	0.156
Computation time[min]	447

viii) IACS design, cone ice hitting on frame area

The ice started hitting the hull at an initial speed of 1.5m/s, and bounced at the speed of 0.46m/s. The maximum stress exceeded the yield strength, and the structure entered the plastic deformation. The maximum equivalent plastic stress was 0.196, happening on the frame, under the failure criteria, and no damage occurred in the process

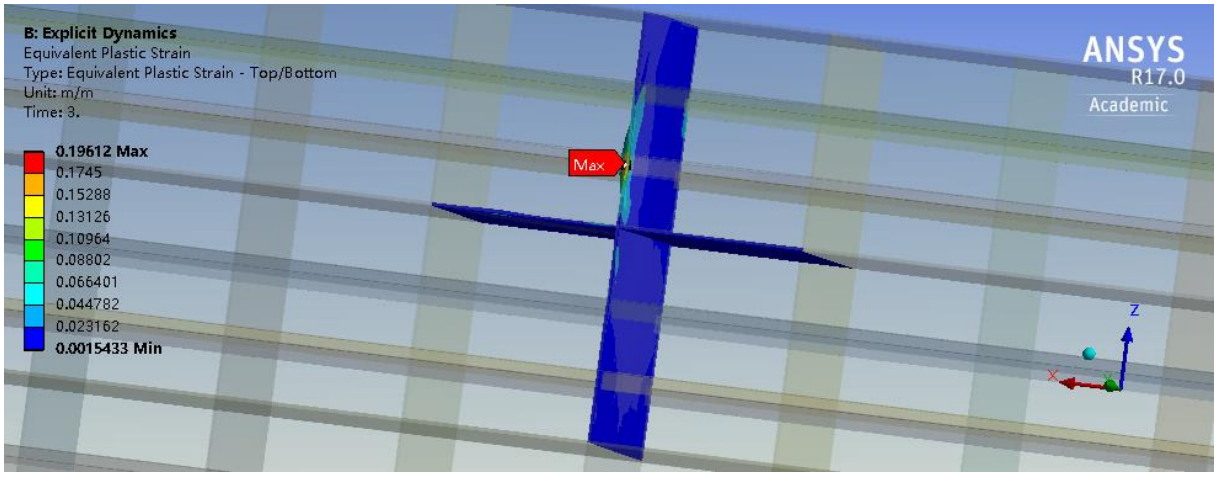

a. frame strain distribution

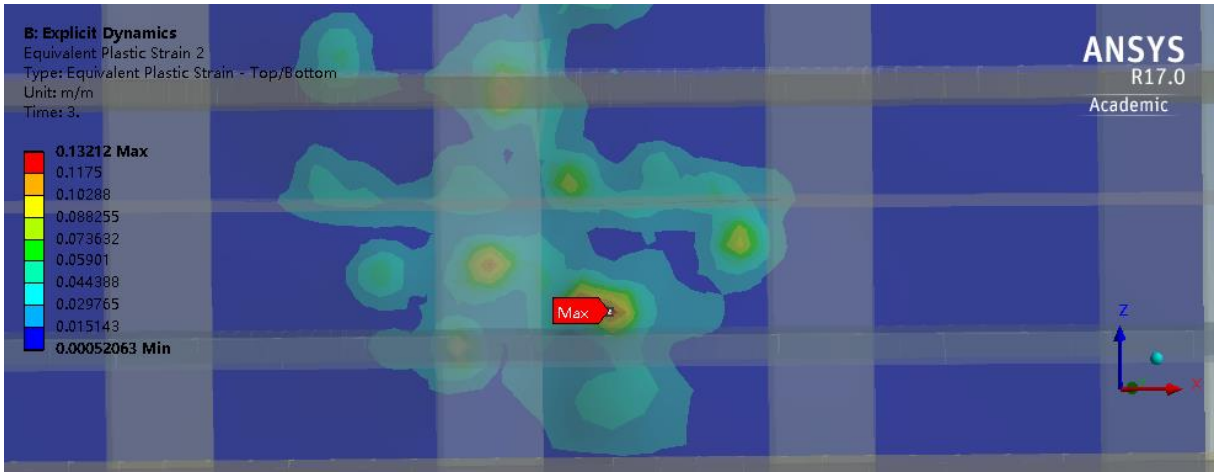

b. plate strain distribution

Figure A-8 Final equivalent plastic strain distribution of IACS design, cone ice, frame area

Table A-8 Simulation results of IACS design, cone ice, frame area

Object	value
Ice initial speed[m/s]	1.5
Bounced speed[m/s]	0.46
Ice mass[t]	3169

(Continued Table A-8)

Object	value
Kinetic energy loss[J]	3215576
Damage area on plate[m^2]	0
Damage area on frame[m^2]	0
Maximum deformation on plate[m]	0.238
Maximum deformation on frame[m]	0.149
Computation time[min]	536

A.3 With forward speed

ix) FSICR design, bullet ice with foreword speed

The maximum strain was around the start point, where the contact area was the least. Although the local collision was not critical and the equivalent plastic strain was far from damage, two plastic deformation area were obvious.

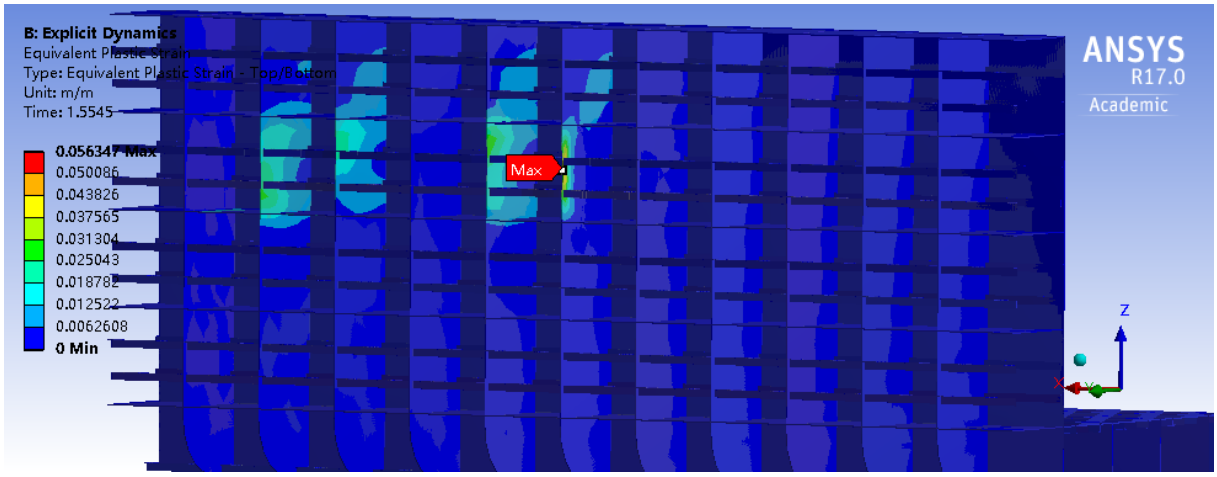

a. frame strain distribution

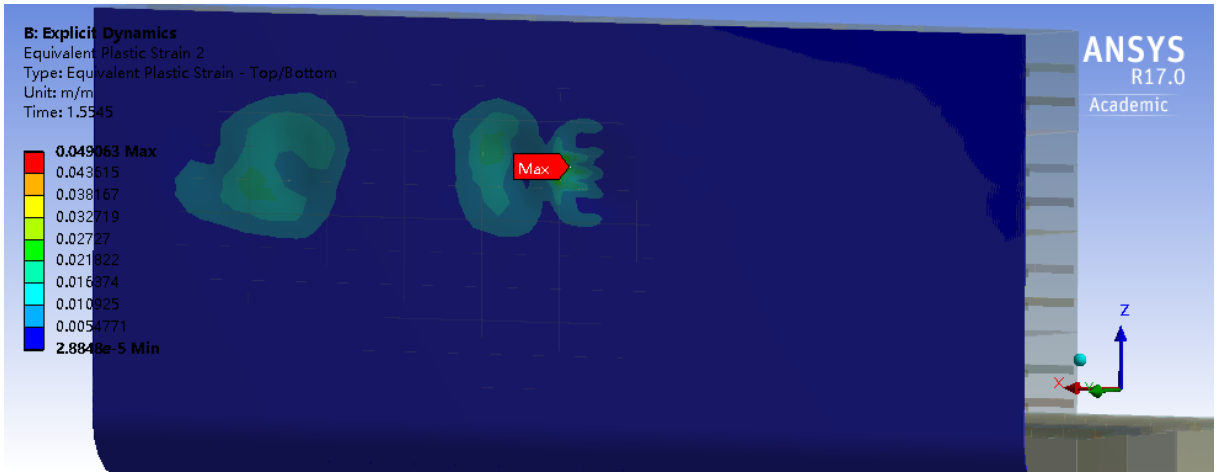

b. plate strain distribution

Figure A-9 Final equivalent plastic strain distribution of FSICR design, bullet ice with forward speed

Table A-9 Simulation results of FSICR design, bullet ice with forward speed

Object	value	
Ice initial speed[m/s]	U_x	U_y
	10	-1.5

(Continued Table A-9)

Object	value	
Bounced speed[m/s]	U_x	U_y
	10	-1.0
Ice mass[t]	3169	
Damage area on plate[m^2]	0	
Damage area on frame[m^2]	0	
Maximum deformation on plate[m]	0.207	
Maximum deformation on frame[m]	0.137	
Computation time[min]	290	

x) IACS design, bullet ice with foreword speed

The same as case ix, the maximum strain was around the start point, where the contact area was the least. The value was much lower than case I to xiii.

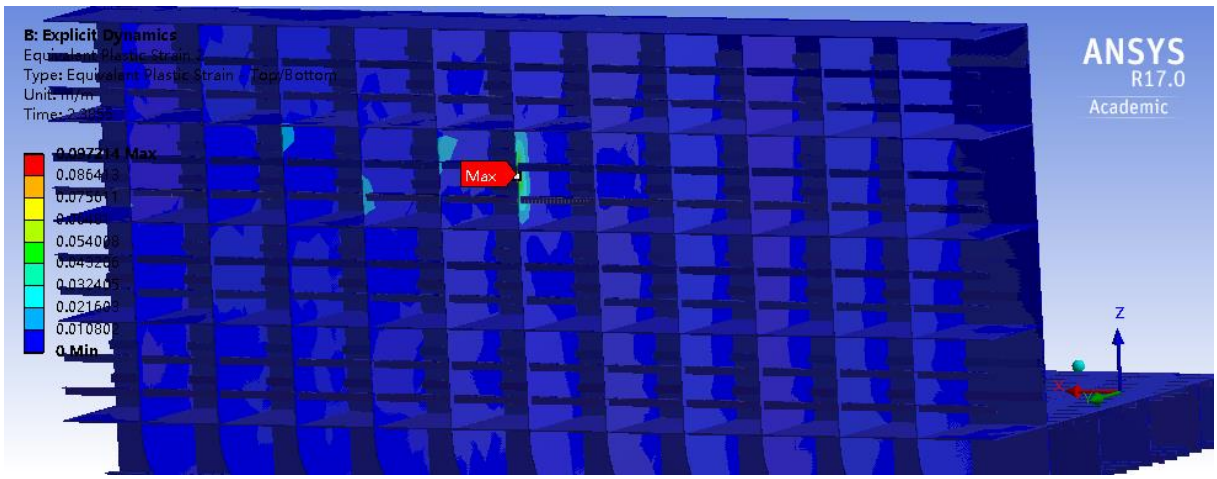

a. frame strain distribution

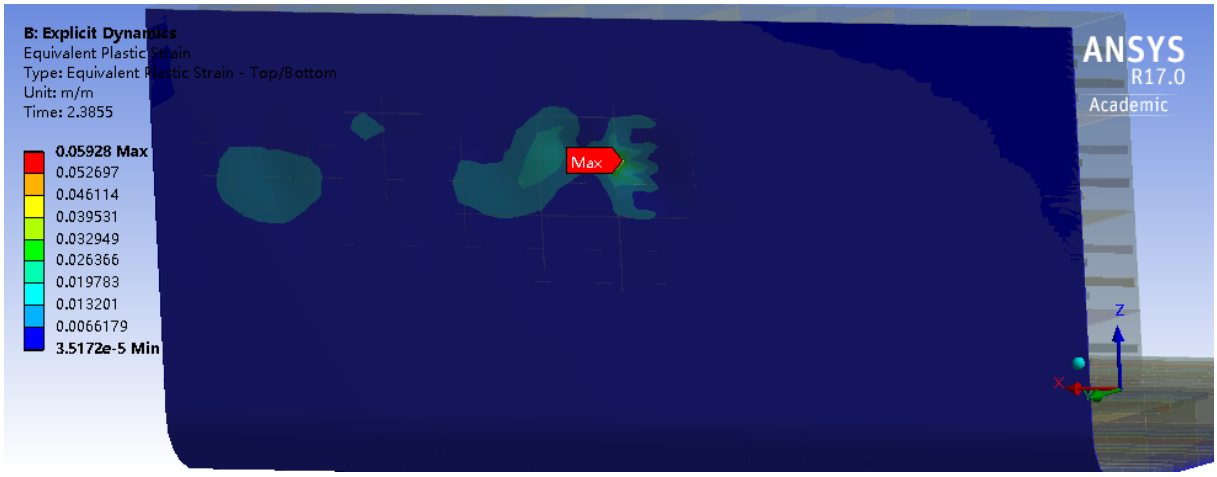

b. plate strain distribution

Figure A-10 Final equivalent plastic strain distribution of IACS design, bullet ice with forward speed

Table A-10 Simulation results of IACS design, bullet ice with forward speed

Object	value	
Ice initial speed[m/s]	U_x	U_y
	10	-1.5
Bounced speed[m/s]	U_x	U_y
	10	-1.1
Ice mass[t]	3169	

(Continued Table A-10)

Object	value
Damage area on plate[m^2]	0
Damage area on frame[m^2]	0
Maximum deformation on plate[m]	0.178
Maximum deformation on frame[m]	0.142
Computation time[min]	349

xi) FSICR design, cone ice with foreword speed

The maximum was at the edge of the hull, because of the randomness of the collision process. Though the strain value was lower than bullet ice (case ix), the plastic deformation area was much more than case ix and x.

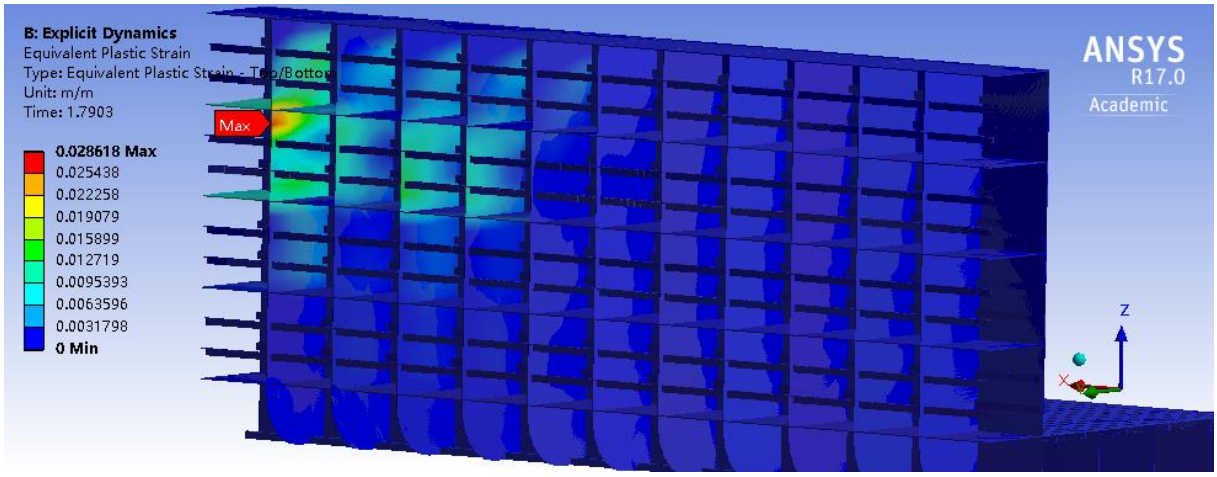

a. frame strain distribution

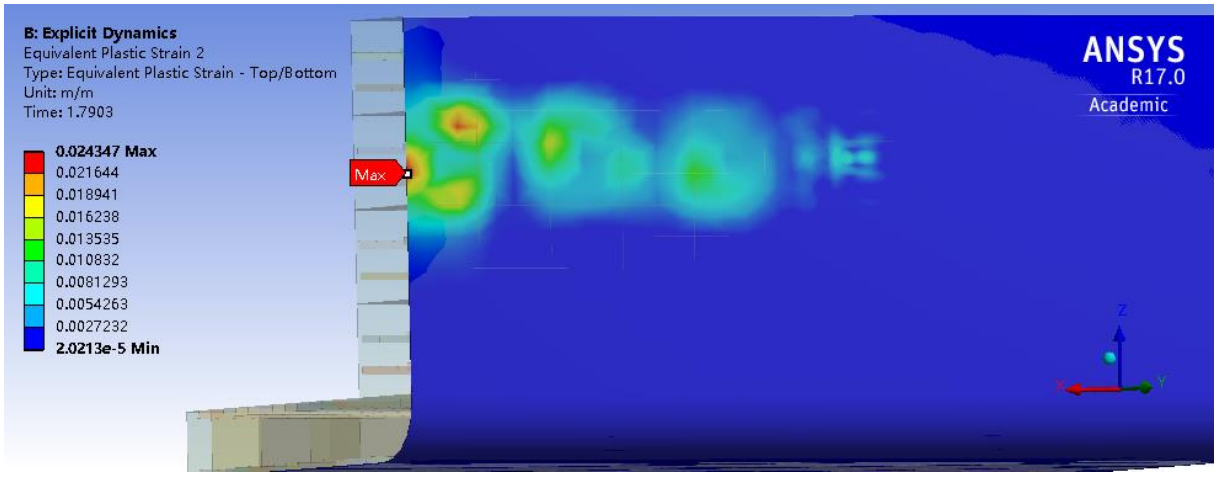

b. plate strain distribution

Figure A-11 Final equivalent plastic strain distribution of FSICR design, cone ice with forward speed

Table A-11 Simulation results of FSICR design, cone ice with forward speed

Object	value	
Ice initial speed[m/s]	U_x	U_y
	10	-1.5
Bounced speed[m/s]	U_x	U_y
	10	-1.02

(Continued Table A-11)

Object	value
Ice mass[t]	3155
Damage area on plate[m^2]	0
Damage area on frame[m^2]	0
Maximum deformation on plate[m]	0.183
Maximum deformation on frame[m]	0.068
Computation time[min]	287

xii) IACS design, cone ice with foreword speed

This case was similar to case xi with a lower strain value.

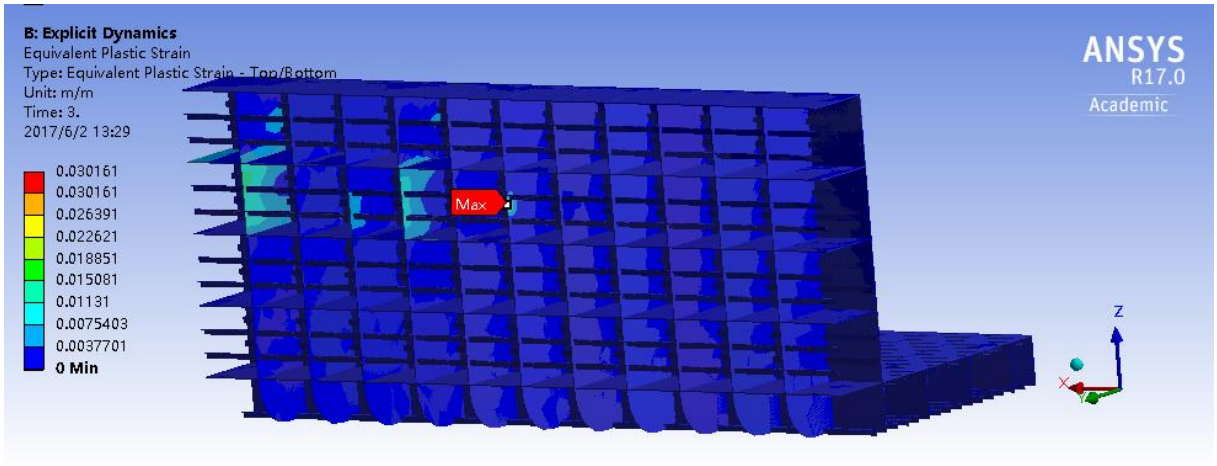

a. frame strain distribution

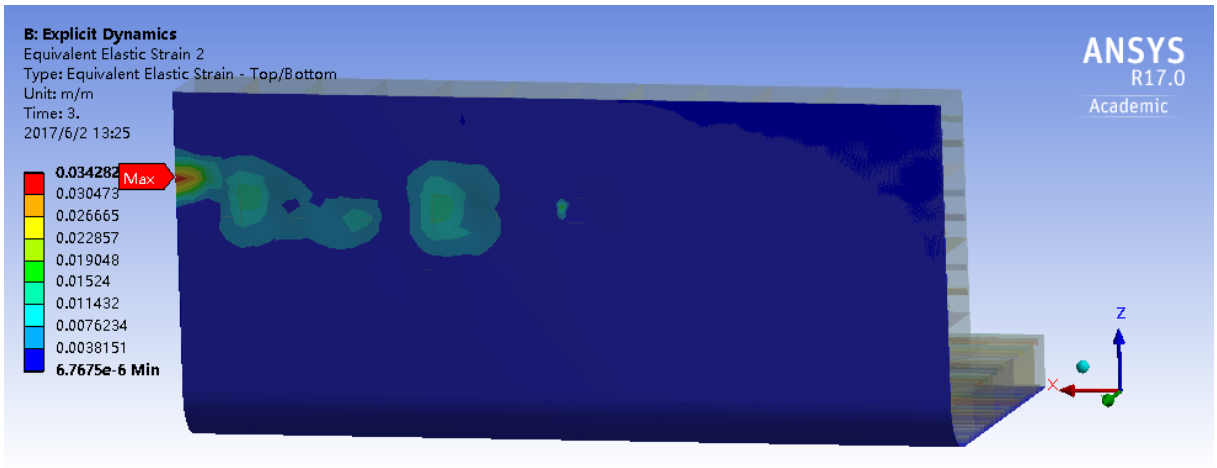

b. frame strain distribution

Figure A-12 Final equivalent plastic strain distribution of IACS design, cone ice with forward speed

Table A-12 Simulation results of IACS design, cone ice with forward speed

Object	value	
Ice initial speed[m/s]	U_x	U_y
	10	-1.5
Bounced speed[m/s]	U_x	U_y
	10	-1.23
Ice mass[t]	3155	
Damage area on plate[m^2]	0	

(Continued Table A-12)

Object	value
Damage area on frame[m^2]	0
Maximum deformation on plate[m]	0.137
Maximum deformation on frame[m]	0.042
Computation time[min]	302

List of Figures

List of Tables